Intersubunit Electrostatic Complementarity in the RecA Nucleoprotein Filament Regulates Nucleotide Substrate Specificity and Conformational Activation†

Andrew M. Lee and Scott F. Singleton*

School of Pharmacy, Division of Medicinal Chemistry & Natural Products, University of North Carolina at Chapel Hill, CB #7360, Chapel Hill, North Carolina 27599-7360

Received November 9, 2005; Revised Manuscript Received February 7, 2006

ABSTRACT: The *Escherichia coli* RecA protein is the prototypical member of a family of molecular motors that transduces ATP binding and hydrolysis for mechanical function. While many general mechanistic features of RecA action are known, specific structural and functional insights into the molecular basis of RecA activation remain elusive. Toward a more complete understanding of the interdependence between ATP and DNA binding by RecA, we report the characterization of a mutant RecA protein wherein the aspartate residue at position 100 within the ATP binding site is replaced by arginine. Physiologically, D100R RecA was characterized by an inducible, albeit reduced, activation of the SOS response and a diminished ability to promote cellular survival after UV irradiation. Biochemically, the D100R substitution caused a surprisingly modest perturbation of RecA−ATP interactions and an unexpected and significant decrease in the affinity of RecA for ssDNA. Moreover, in vitro assays of RecA activities requiring the coordinated processing of ATP and DNA revealed (1) a 2−5-fold decrease in steady-state turnover of ATP; (2) no formation of mixed nucleoprotein filaments when wild-type and D100R RecA compete for limiting ssDNA; and (3) no formation of strand exchange reaction products. Taken together, these results suggest that the D100R mutational effects on isolated RecA activities combine synergistically to perturb its higher-order functions. We conclude that the replacement of Asp100 resulted in a change in the electrostatic complementarity between RecA monomers during active filament assembly that prevents the protein from fully accessing the active multimeric state.

The *Escherichia coli* RecA protein catalyzes an ATP-dependent DNA strand exchange reaction that is crucial to the physiologic processes of homologous recombination and recombinational DNA repair (*1*, *2*). In this context, RecA is thought to function as a molecular motor that transduces ATP binding energy via ligand-dependent conformational changes to the DNA rotations that allow strand exchange (*3*, *4*). Indeed, RecA is the prototypical member of a family of proteins that transduce the energy of ATP binding for mechanical function. The RecA core domain, which includes the site of ATP binding and hydrolysis (*5*, *6*), can be considered a fundamental component of other motor proteins such as the F_1 ATPase (*7*) and hexameric nucleic acid helicases (*8*−*10*). Because the structure of the RecA core domain is conserved across a wide variety of ATP-binding motor proteins, characterization of the structural and functional mechanisms of activation of RecA will undoubtedly enhance our understanding of the mechanistic details associated with the family of RecA-like ATPases.

Unlike other motor proteins, RecA is active only as a helical filament in complex with both DNA and ATP. Multiple RecA monomers cooperatively bind ssDNA[1] sequence-independently, stoichiometrically coating the ssDNA, and forming a multimeric right-handed helical nucleoprotein filament with about 6 RecA monomers and 18 DNA nts per helical turn. EM defined two conformations of the RecA nucleoprotein filament with helical pitches of ∼70 or ∼95 Å (*11*). The collapsed and extended filaments bind DNA with different affinities, the collapsed filament representing a low-affinity conformation, whereas the extended filament is a high-affinity conformation. The conformational state of the NPF, and its relative affinity for DNA, is controlled by adenosine nucleotides. The collapsed, low-affinity filament forms when ADP is present, whereas the extended, high-affinity filament forms with ATP or its isosteres such as ATPγS (*12*). All available evidence is consistent with the conclusion that the extended NPF comprising RecA protein, ssDNA, and ATP(γS) is the active state of RecA, which forms the recombination machinery that pairs and exchanges homologous DNA strands (*13*, *14*) and serves as the initiating signal for induction of the SOS response (*15*). Although a wealth of information is available on the structure of the RecA protein itself (*16*−*18*), a high-resolution structure of the extended, active conformation of RecA has remained elusive.

† This work was supported by a grant to S.F.S. from the National Institutes of Health (GM58114).

* To whom correspondence should be addressed. Tel: 919-966-7954. Fax: 919-966-0204. E-mail: sfs@unc.edu.

[1] Abbreviations: 6MI, 6-methylisoxanthopterin; ATPγS, adenosine-5′-*O*-(thiotriphosphate); dsDNA, double-stranded DNA; EM, electron microscopy; GTP, guanosine-5′-triphosphate; ITP, inosine-5′-triphosphate; MANT-ADP, 2′(3′)-*O*-(*N*-methylanthraniloyl)adenosine-5′-diphosphate; MESG, 2-amino-6-mercapto-7-methyl guanine; NPF, nucleoprotein filament; nts, nucleotides; ODN, oligodeoxyribonucleotide; SSB, single-stranded DNA binding protein; ssDNA, single-stranded DNA.

10.1021/bi052296x CCC: $33.50
Published on Web 03/18/2006

In part as a result of this lack of structural information, the molecular determinants for many of RecA's physiologic mechanisms are not fully understood, and many deceptively simple questions remain to be answered (*18*, *19*). One such question that has been of recent interest to us (*20*, *21*) as well as others (*18*, *22*−*25*) is how ATP and ssDNA binding are structurally and functionally coupled to give rise to the cooperative allosterism in ligand binding and processing that are characteristic of RecA's activities. Toward this end, VanLoock et al. recently reported an 18-Å EM reconstruction of the extended NPF from which they developed a pseudoatomic model of the active state of RecA (*25*). Relative to their positions in the crystal structures of compressed, inactive filaments, the subunits in the structural model for the active, extended RecA filament underwent rotations that bring the ATP binding site of one RecA monomer into close proximity with the neighboring monomer. The location of the site of ATP binding and hydrolysis at the subunit interface provides insight into the structural basis for the observed cooperative hydrolysis of ATP.

Recently, we have explored the relative abilities of canonical nucleotides and their synthetic analogues to activate or inhibit the formation of RecA nucleoprotein filaments (*20*, *21*, Wigle et al., in press). In this context, we were inspired by the report from the Bryant laboratory that replacing the Asp100 residue with Asn altered the nucleotide preference of RecA from ATP to ITP (*26*, *27*). This functional specificity change was presumed to arise from changes in the interactions between the side chain at position 100 and the exocyclic functional group at position 6 of the purine ring. In an effort to exploit this observation to expand the repertoire of nucleotide analogues utilized as substrates by RecA, we created a small library of Asp100 mutant RecA proteins (D100X) and screened the library for in vitro and in vivo activity. On the basis of these results, the D100R RecA protein was selected for more careful characterization.

As described herein, our data with the D100R RecA are inconsistent with a role for the aspartate at position 100 that is limited to controlling the NTP specificity of RecA. Rather, in the context of the VanLoock et al. pseudoatomic model for the active conformation of the RecA nucleoprotein filament, our data are consistent with the hypothesis that subunit rotation occurs during activation, and suggest that changes in residues traditionally ascribed to the NTP binding site can impact the higher-order functions of RecA. We further hypothesize that conformational activation depends on electrostatic complementarity across the subunit interface and that RecA uses Coulomb forces to transduce NTP binding to effect both protein conformational change and high-affinity DNA binding, which are required for formation of the active RecA nucleoprotein filament.

EXPERIMENTAL PROCEDURES

Materials. Circular ϕX174 cssDNA and dsDNA were from New England Biolabs. The poly(dT) ssDNA (average length = 319 nts) was purchased from Amersham Biosciences, SSB was purchased from Promega, ATP and ATPγS were purchased from Roche, and MANT-ADP was purchased from Molecular Probes. Unless otherwise indicated below, all other reagents were purchased from Sigma at the highest purity available.

Generation of Asp100 Mutant RecA Library. A small library of RecA proteins with a mutation at aspartic acid 100 was generated using QuikChange site-directed mutagenesis (Stratagene). A pBluescriptII (KS+) plasmid containing the RecA gene was used as a template in a QuikChange PCR reaction with a primer, 5′-CGCGCTG**NN**CCCAATCTACG-CACGTAAACTGGGCGTCGACATCGACAACC-3′, and its complement, where **N** is any of the four nucleobases. The D100K, D100Q, and D100N mutants were obtained using a primer, 5′-CGCGCTG**M**A**K**CCAATCTACGCACGTAAA-CTGGGCGTCGACATCGACAACC-3′, and its complement, where **M** is adenosine or cytidine, and **K** is thymidine or guanosine. The resulting PCR products were used to transform DH5α cells (Invitrogen), and the plasmids were isolated from cultures of these cells and sequenced. The genes with the desired sequences were subcloned into the pTrc99A vector (Amersham Biosciences) for in vivo assays of RecA function (*28*), or into the pTXB3 vector (New England Biolabs) for protein expression and purification (*29*).

Small-Scale Purification and Preliminary Biochemical Analysis of Mutant RecA Proteins. The *E. coli* RecA protein and 12 D100X RecA proteins were purified using the "Small-scale *C*-terminal fusion protein expression and purification" protocol previously described (*29*) and stored in aqueous buffer (25 mM Tris·HCl, pH 7.5, 1 mM DTT, and 5% glycerol) at −80 °C. Protein concentration was determined spectrophotometrically using an extinction coefficient at 280 nm of 2.2×10^4 $M^{-1}\cdot cm^{-1}$ (*30*). In vitro characterization of each protein's ssDNA-dependent ATP hydrolysis activity was carried out as described below.

In Vivo Assay of SOS Induction. Assays of the SOS induction ability of a small library of Asp100 RecA mutant proteins were performed essentially as described previously (*28*, *31*). Briefly, GY7313 cells (*32*) containing the mutant *recA* gene on a plasmid derived from the pTrc99A plasmid (Amersham Biosciences) were grown to saturation overnight. The saturated culture was inoculated into 5 mL of fresh LB-ampicillin media and grown to an $OD_{600} > 0.6$. Cells were diluted to $OD_{600} = 0.3$ in 2 mL of LB in the presence or absence of 0.5 $\mu g\cdot mL^{-1}$ mitomycin C to stimulate DNA damage. After 2.5 h incubation at 37 °C, 2 mL of cells was pelleted in 1.5 mL Eppendorf tubes and resuspended in 0.5 mL of Z buffer (60 mM Na_2HPO_4, 40 mM NaH_2PO_4, 10 mM KCl, 1 mM $MgSO_4$, and 50 mM 2-mercaptoethanol, at pH 7.0). The cells were lysed by sonication (10 pulses, 75W) and spun down at 10 000 rpm for 1 min at 4 °C to remove the membrane fraction. The clarified lysate was removed to a new 1.5 mL Eppendorf tube and assayed for ONPG cleavage and protein concentration.

ONPG cleavage was measured in a 96-well microplate. To each well was added 50 μL of Z buffer, 50 μL of clarified lysate, and 20 μL of 4 $mg\cdot mL^{-1}$ ONPG. Reactions were incubated at room temperature for 6 min to cleave ONPG and were quenched with 50 μL of 1 M Na_2CO_3. The absorbance was recorded at 405 nm using a PerkinElmer HTS7000+ BioAssay Reader equipped with a 405 ± 10 nm band-pass filter (Corion). Total protein concentration was determined by Bradford assay using Bio-Rad Protein Assay reagent in a 96-well microplate format with a 595 ± 25 nm filter.

In Vivo Assay of UV Survival. Assays of the ability of the Asp100 mutant RecA proteins to promote survival to

increasing levels of UV radiation were performed essentially as described (*33*−*35*). ENZ280 cells (*36*) containing the mutant *recA* gene on the pTrc99A plasmid were grown overnight to saturation. The saturated culture was used to inoculate fresh 5-mL LB-ampicillin cultures to grow to $OD_{600} > 0.6$. These cultures were diluted to $OD_{600} = 0.4$ in 10 mM $MgSO_4$ (final volume of 2 mL) and were exposed to varying levels of UV light. Cells were spotted on a gridded LB-ampicillin agar plate and grown overnight. Colony counts were used to compare the survival of the cells containing the different mutant proteins at different UV exposure levels.

Large-Scale Protein Purification. The *E. coli* RecA protein and the D100R mutant RecA protein were purified as described (*29*) to ≥97% homogeneity and stored in aqueous buffer (25 mM Tris·HCl, pH 7.5, 1 mM DTT, and 5% glycerol) at −80 °C. The protein concentrations were determined using the monomer extinction coefficient 2.2×10^4 $M^{-1}\cdot cm^{-1}$ at 280 nm (*30*). Endonuclease (single- and double-stranded DNA) and exonuclease tests, performed as described (*29*), revealed no detectable nuclease contamination in either protein sample.

Characterization of ssDNA-Dependent ATP Hydrolysis Activity. The ssDNA-dependent ATPase activity was measured using an enzyme-coupled assay system essentially as described (*28*, *37*). For poly(dT)-dependent activity, assays were conducted at 37 °C in 600 μL of aqueous buffer containing 1.0 μM RecA protein, 2.3 mM phosphoenolpyruvate, 5 $U\cdot mL^{-1}$ pyruvate kinase, 5 $U\cdot mL^{-1}$ lactic dehydrogenase, 2 mM NADH, and 3 mM ATP in 1× Reaction Buffer (25 mM Tris·HOAc, pH 7.5, at 25 °C, 5% (v/v) glycerol, and 1 mM DTT) with varying concentrations of poly(dT) ssDNA. For ϕX174 cssDNA-dependent activity, assays were conducted under the same conditions except that the DNA concentration was fixed at 8 μM-nts ϕX174 cssDNA and the RecA concentration was varied. The 380-nm absorbance of each solution was recorded every 30 s using a PerkinElmer Lambda 20 UV−Vis Spectrophotometer. The reaction velocity ($\mu M\cdot min^{-1}$) for each ssDNA or RecA concentration was calculated using the measured slope of the NADH absorbance profile (dA/dt) with 1.21 $mM^{-1}\cdot cm^{-1}$ as the extinction coefficient of NADH at 380 nm as previously described (*38*). For the data presented in Table 1, proteins were purified on a small scale to rapidly obtain all proteins in the library for activity assays. ATPase assays of these proteins were performed as described above with modifications for 96-well microplate format. WT and D100R RecA were subsequently purified on a large scale for all other experiments described and assayed for ATPase activity as described above.

The data were fit with the following equation to determine the velocity of the reaction and the DNA binding stoichiometry value:

$$v_{obs}^0 = \frac{V_{max}}{2}\cdot\left(R_0 + \frac{D_0}{n} + K_d - \sqrt{\left(R_0 + \frac{D_0}{n} + K_d\right)^2 - \left(4R_0\frac{D_0}{n}\right)}\right) \quad (1)$$

where V_{max} is the maximum velocity of the reaction, R_0 is the total concentration of protein in the reaction, D_0 is the total DNA concentration in nucleotides, n is the DNA/RecA stoichiometry (nts per monomer), and K_d is the apparent dissociation constant for DNA binding (usually set to zero). For the D100R data, a different equation was used to determine the ATPase parameters, as follows:

$$v_{obs}^0 = \frac{V_{max}\left(\frac{c}{C_{0.5}}\right)^n}{1 + \left(\frac{c}{C_{0.5}}\right)^n} \quad (2)$$

where V_{max} is the maximum velocity of the reaction, c is the independent variable (either [RecA] or [DNA] for the ϕX174- or poly(dT)-dependent assays, respectively), n is the apparent cooperativity in RecA−DNA binding, and $C_{0.5}$ is the concentration of titrant at which the velocity is half-maximal. The steady-state turnover number for ATP hydrolysis can then be calculated using $k_{cat} = V_{max}/R_0$.

Characterization of Steady-State Kinetic Parameters for NTP Turnover. The binding of NTPs to RecA protein was measured using an enzyme-coupled assay system for monitoring P_i release (*39*) with modifications for use in a 96-well format. Assays were conducted at 37 °C in 100 μL of aqueous buffer containing 0.5 μM RecA protein, 15 μM nts poly(dT), 1 $U\cdot mL^{-1}$ purine nucleoside phosphorylase, 0.2 mM MESG, 25 mM Tris·HOAc, pH 7.1, 10 mM $Mg(OAc)_2$, 1 mM DTT, 5% (v/v) glycerol, and various concentrations of NTP. The NTP being assayed was serially diluted to yield various concentrations at 10× final concentration in 100 mM $Mg(OAc)_2$. These solutions served as the start solution for the assay reactions. To each well of a flat-bottom 96-well microplate was added 10 μL of the appropriate NTP/$Mg(OAc)_2$ solution. The remaining assay components were combined in a total volume of 90 μL and added to each well containing NTP and $Mg(OAc)_2$. The 360-nm absorbance of each solution was recorded every 15 s using a PerkinElmer HTS7000+ BioAssay Reader equipped with a 360 ± 10 nm band-pass filter (Andover Corp.). The reaction velocity ($\mu M\cdot min^{-1}$) for each NTP was calculated from the change in absorbance as a function of time (dA/dt) using the change in extinction coefficient, $\Delta\epsilon = 6.0 \times 10^{-4}$ μM^{-1}, as measured in the microplate reader.

Each set of data, corresponding to a range of NTP concentrations, was analyzed using a Michaelis−Menten equation modified for substrate cooperativity

$$v_{obs}^0 = \frac{V_{max}}{[NTP]^{n_H} + S_{0.5}^{n_H}} \quad (3)$$

where V_{max} is the reaction velocity at saturation, $S_{0.5}$ is the [NTP] when the velocity is half of its maximum value, and n_H is the Hill coefficient (*40*, *41*).

Fluorescence Studies of MANT-ADP Binding by RecA. The binding of the fluorescent nucleotide analogue MANT-ADP to WT and D100R RecA proteins was measured using a QuantaMaster-6 steady-state spectrofluorometer (Photon Technology International, Lawrenceville, NJ) in T-format using 2 × 10 mm I-beam quartz cuvettes. A solution containing 1× Reaction Buffer, 4 mM $Mg(OAc)_2$, and 1.5 μM MANT-ADP was added to a cuvette, and the cuvette was placed in the fluorometer with the cell holder temperature set to 37 °C. The solution was incubated for 5 min in

the cell holder, and the fluorescent emission was recorded from 390 to 490 nm with excitation at 356 nm and a 4-nm slit width. The 2-mm path length of the I-beam cuvette was used for excitation to minimize the inner filter effect. Small aliquots of protein were added to the cuvette, and the solution was incubated for 5 min at 37 °C after each addition before measurement of the fluorescent emission. Parallel and perpendicular emissions were collected simultaneously using Glan-Thompson polarizers on both the excitation and emission beams. The excitation polarization was set to 0°, with the emission channels set to 0 and 90° for parallel and perpendicular collection, respectively. Total emission and anisotropy were reconstructed from the parallel and perpendicular channel data in the usual manner: $I_{tot} = I_{ll} + 2{\cdot}I_{\perp}$; $r = (I_{ll} - I_{\perp})/(I_{ll} + 2{\cdot}I_{\perp})$.

To determine the K_d of MANT-ADP binding by the RecA proteins, the total intensity data was fit with the following equation:

$$I = I_0 + \left(\frac{\Delta I}{3}\right)\left(R + \frac{D_0}{n} + K_d - \sqrt{\left(R + \frac{D_0}{n} + K_d\right)^2 - 4R\frac{D_0}{n}}\right) \quad (4)$$

where I_0 is the initial fluorescence (set at 1 for the normalized total intensity data), ΔI is the total change in fluorescence, R is the protein concentration, and K_d is the dissociation constant for the RecA protein with MANT-ADP. The best fit of the data was obtained with $D_0/n = 1.5$.

Fluorescence Studies of DNA Binding by RecA Proteins. The binding of WT and D100R RecA to ssDNA was measured using a 30mer ssDNA labeled with the 6MI fluorophore (*20*, *42*, *43*) in a 2-mm × 10-mm I-beam cuvette. Fluorescence data were collected using 3 μM nts labeled 30mer ssDNA and (when added) 100 μM ATPγS in 1× Reaction Buffer with 4 mM $Mg(OAc)_2$ at 37 °C. The 2-mm path length of the I-beam cuvette was used for excitation to minimize the inner filter effect. The fluorophore was excited at 340 nm with a 4-nm slit width, and parallel and perpendicular emissions were recorded simultaneously through monochromators using the T-format of the fluorometer with Glan-Thompson polarizers on the excitation and emission beams, as for the experiments with MANT-ADP detailed above. Small aliquots of RecA protein were added to the reaction solution, and emission spectra were collected from 390 to 470 nm after incubation of each addition for 5 min at 37 °C.

For binding in the absence of ATPγS, the total intensity data were fit using eq 5

$$F = F_0 + \left(n\frac{\Delta F}{D_0}\right)\left(R_o + \frac{D_0}{n} + K_d - \sqrt{\left(R_0 + \frac{D_0}{n} + K_d\right)^2 - 4R_0\frac{D_0}{n}}\right) \quad (5)$$

where F is the observed fluorescence, F_0 is the initial fluorescence value (fixed at 1 for normalized total intensity fits), ΔF is the change in the fluorescence property, n is the DNA/RecA stoichiometry (fixed at 3 for these data), D_0 is the initial DNA concentration (3 μM nts for these experiments), R_0 is the concentration of protein at each titration point, and K_d is the dissociation constant for DNA binding by the RecA protein.

Total intensity data obtained in the presence of ATPγS exhibited a more sigmoidal trend than in the absence of ATPγS, and was fit with a binding isotherm equation that contained a cooperativity parameter as follows:

$$F = 1 + \frac{\Delta F\left(\left(\frac{R_0}{K_d}\right)^m\right)}{1 + \left(\frac{R_0}{K_d}\right)^m} \quad (6)$$

where F is the total intensity, ΔF is the change in intensity, R_0 is the protein concentration, K_d is the dissociation constant for DNA binding, and m is the cooperativity factor for binding.

DNA Three-Strand Exchange Assays. Strand exchange promoted by the WT and D100R RecA proteins was monitored essentially as described (*44*, *45*). RecA was incubated at 37 °C for 10 min at 10 μM final concentration with 20 μM nts ϕX174 cssDNA in 1× Reaction Buffer with 10 mM $Mg(OAc)_2$, 12 mM phosphocreatine, and 10 U·mL^{-1} creatine phosphokinase. After the initial incubation, ϕX174 linear dsDNA (form III) was added to 20 μM nts final concentration, and the mixture was incubated for another 10 min at 37 °C. During this second incubation, 10 μL was removed as the 0 min aliquot and added to 3.3 μL of RecA stop dye (60 mM EDTA, 5% (w/v) SDS, 25% (v/v) glycerol, and 0.2% bromophenol blue) to inactivate the RecA and stop the strand exchange reaction. A cocktail of ATP and SSB was added to the reaction to a final concentration of 3 mM ATP and 2 μM SSB, and the reaction was allowed to proceed at 37 °C. Aliquots were taken by removal of 10 μL at 10, 30, 60, and 90 min after the addition of ATP. The aliquots were run on a 0.8% agarose gel for 12 h at 30 V, and the gel was stained for 1.5 h with 1× SYBR Gold (Molecular Probes) for visualization.

Molecular Model Building for Active Filament Conformation. The all-atom model of the active RecA filament was constructed by superimposing the C_α backbone of the Xing and Bell crystal structure (PDB code 1XMV; (*46*)) onto the C_α backbone of two adjacent RecA-filament subunits of the Egelman laboratory electron microscopy model of the active filament (PDB code 1N03; (*25*)). A simple minimization of the superimposed, all-atom structure was then performed using Insight II (Accelrys) to relieve steric clashes between residues due to adjustments in their position made during alignment.

RESULTS

Design and Preparation of a Purified D100X RecA Library. To explore the permissiveness of Asp100 to substitution, we created a small library of *recA* genes with Ser, Thr, Asn, Gln, Gly, Ala, Val, Ile, Phe, Pro, Lys, or Arg codons replacing that of Asp100. Our previous studies of mutant RecA proteins began with in vivo activity assays prior to performing laborious purification procedures (*28*). However, we recently established a rapid RecA purification strategy that yields a final RecA solution with a suitable concentration (>20 μM) for immediate use in biochemical

assays in vitro(*29*). As such, we elected to purify all the mutant RecA proteins simultaneously and initiate our studies with in vitro biochemical assays of the mutant proteins' activities. Purifications of the RecA mutants listed above were performed in parallel on a small-scale as described (*29*). The average yield for the small-scale purification was 1.5 mg of protein, and the proteins were determined to have purities >94%.

In Vitro ATPase Activities of the D100X RecA Proteins. The first step in both DNA strand exchange and repressor cleavage is the binding of RecA to ssDNA and ATP to form an active, extended nucleoprotein filament. The filament formed by WT RecA with ssDNA and ATP results in ATP hydrolysis such that this activity serves as a useful indicator of active nucleoprotein filament formation. Therefore, we tested the abilities of the D100X RecA proteins to hydrolyze ATP in the presence of ssDNA. The ssDNA-dependent ATPase activities were measured using a coupled enzyme spectrophotometric assay essentially as described (*28*). The maximum initial rates are summarized graphically in Figure 1 for the proteins in assays with poly(dT) ssDNA (Figure 1A) and ϕX174 cssDNA (Figure 1B).

In one set of experiments, initial rates of ATP hydrolysis were measured using excess poly(dT) to activate either the WT or D100X RecA protein (1 μM). The initial hydrolysis rates depended not only on the concentration of poly(dT) present but also on the identity of the protein (data not shown). However, the v_{obs}^0 data for each protein reached a maximum value at or slightly above a ratio of three nucleotides per RecA monomer, and increasing the poly(dT) concentration resulted in no further rate increase. The kinetic V_{max} parameters, each obtained by horizontal linear fits of the v_{obs}^0 data at high [poly(dT)] for the individual proteins, were comparatively evaluated at this point (Figure 1). Analysis of the data for WT RecA yielded $V_{max} = 19$ μM·min^{-1}. The small difference between this value and those reported previously (*28*, *37*, *47*) likely results from the fact that protein samples prepared using the rapid, small-scale method have slightly lower physical purities (>94% vs >97%) (*29*). Although the rapid, small-scale purification procedure is not suitable for quantitative comparisons, it is acceptable for analyzing relative differences. Yielding relative V_{max} values within the range 50−75% that of WT RecA, the mutant RecA proteins having small, polar, or charged residues (i.e., Gly, Ala, Ser, Thr, Asn, Gln, Lys, and Arg) in place of Asp100 were nearly as active as WT RecA. In contrast, no ATP hydrolysis was catalyzed by the mutant RecA proteins having Val, Ile, Phe, or Pro in place of Asp100. Our findings with the D100N RecA protein are similar to those from work performed in the Bryant laboratory (*26*, 27), in which they observed that the D100N RecA protein was as active as WT RecA for ssDNA-dependent ATP hydrolysis.

In a second set of experiments, RecA titrations were performed with ϕX174 cssDNA at a fixed concentration of 8 μM nts. As before, the initial hydrolysis rates depended on both the concentration and the identity of the protein present (data not shown). The ATP hydrolysis rates were not sensitive to protein concentrations in excess of those required to saturate the DNA lattice (i.e., 2−3 μM). To compare the relative activities of the RecA protein variants, the concentration-dependent ATPase rates were analyzed as

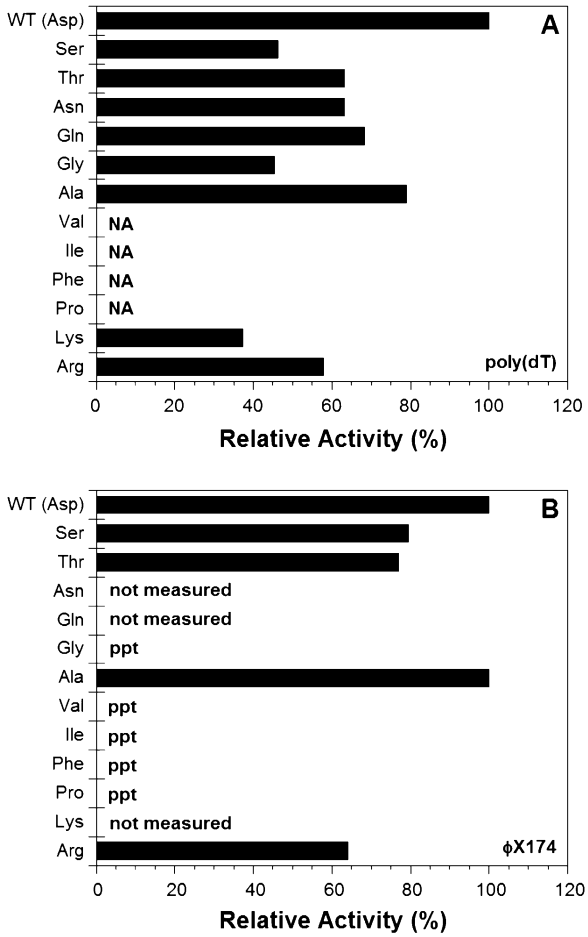

FIGURE 1: ATPase activity of small-scale purified D100X mutant RecA proteins. Comparison of the relative V_{max} of ATP hydrolysis by the D100X mutant RecA proteins is shown in the graphs above. (A) The relative V_{max} for ATP hydrolysis in the presence of poly(dT) ssDNA is shown. The values for V_{max} are displayed as a percentage of the maximum velocity for the WT RecA protein. "NA" indicates that the protein displayed No Activity in the poly(dT)-dependent ATPase assay. (B) The relative V_{max} for ATP hydrolysis in the presence of ϕX174 cssDNA is shown. Values are displayed as in panel A, and "ppt" signifies that a precipitate was observed in the ATPase assays with the indicated proteins. Assays were not performed with D100N, D100Q, and D100K small-scale-purified proteins, as indicated by "not measured".

described above to obtain the kinetic V_{max} parameter for all the proteins. Yielding V_{max} values within the range 55−100% that of the WT protein, the mutant RecA proteins having Ala, Ser, Thr, or Arg in place of Asp100 were only modestly less active than WT RecA. For those mutant RecA proteins that were not activated by poly(dT)—D100V, D100I, D100F, and D100P—as well as for D100G RecA, ϕX174-dependent ATP turnover could not be evaluated because the proteins precipitated from solution at concentrations higher than 1 μM.

In summary, substitution of the nonpolar residues valine, isoleucine, phenylalanine, or proline for Asp100 yielded proteins with no discernible ATPase activity. Moreover, these four mutant proteins and D100G RecA apparently form insoluble aggregates when present at >1 μM in the aqueous buffer used for the ATPase assays. In contrast, the activities of the D100A RecA protein were most similar to those of WT RecA. Similarly, substitution of the polar or charged residues serine, threonine, asparagine, glutamine, lysine, or

arginine for Asp100 gave proteins with somewhat decreased ATP turnover relative to wild-type RecA.

Biological Activities of the D100X RecA Proteins. To characterize further the active D100X mutant RecA proteins, two distinct biological processes involving the RecA nucleoprotein filament were utilized: RecA-mediated induction of the SOS response and RecA-dependent initiation of recombinational DNA repair (*16*). RecA can modulate DNA repair processes by initiating the SOS response in which a collection of gene products under control of the LexA repressor are induced. In the presence of ATP, WT RecA protein bound to ssDNA is activated for coproteolytic cleavage of the LexA protein. To evaluate the abilities of the mutant RecA proteins to induce the SOS response, we measured β-galactosidase activity in GY7313 cells harboring a *lacZ* reporter gene fused to the *sfi* promoter, which is regulated by LexA. RecA-directed coproteolysis of LexA derepresses *lacZ*, and the β-galactosidase produced can be quantitatively measured by an established colorimetric assay. The extent of β-galactosidase induction is therefore an indirect measurement of the RecA protein's ability to form a complex with both DNA and ATP, and the ability of this complex to activate LexA for autoproteolysis (*15*). A reduced activity indicates either a reduced ability to form the quaternary complex or a problem with recognition or cleavage of LexA protein. Alternatively, constitutive coprotease activity can imply stabilization of the active nucleoprotein filament, perhaps due to enhanced ssDNA binding.

β-Galactosidase induction in Δ*recA* bacteria transformed by a plasmid with the WT *recA* gene expressed from the *trc* promoter (Figure 2A) was 10-fold greater than the basal level 2.5 h after treatment of the transformants with mitomycin C. All of the mutant proteins were characterized by *induced* coprotease activities (gray bars) essentially identical to the WT activity (within experimental uncertainty), with the exception of the D100R and D100K mutant proteins. However, the D100A, D100S, D100T, D100N, and D100Q RecA proteins displayed anomalous activity, resulting in the apparent constitutive expression of SOS response elements in the absence of DNA damage (white bars). In contrast, the D100K protein exhibits a markedly decreased ability to mediate repressor coproteolysis, as the levels of induction with the D100K mutant are similar to that of the *recA*$^-$ control strain. In the SOS induction assays, only the arginine substitution (D100R) resulted in inducible coprotease activity similar to that observed for WT RecA (Figure 2A). However, the arginine substitution decreased the extent of SOS induction by approximately 50%.

To investigate the influence of amino acid substitutions for Asp100 on overall DNA repair, we measured the fractional survival after UV irradiation of ENZ280 cells transformed by plasmids carrying WT and mutant *recA* genes. This UV survival assay is a second powerful tool for comparing the relative activities of RecA proteins in vivo. Although the molecular foundations of RecA activity in the UV survival assay are more obscure than those of the LexA coproteolysis assay, it is a sensitive method for discriminating among the activities of the mutant proteins.

Survival curves were constructed to compare the relative abilities of the WT and mutant RecA proteins to repair UV-damaged DNA (Figure 2B). The results mirror those results obtained from the assays of SOS induction. In the survival

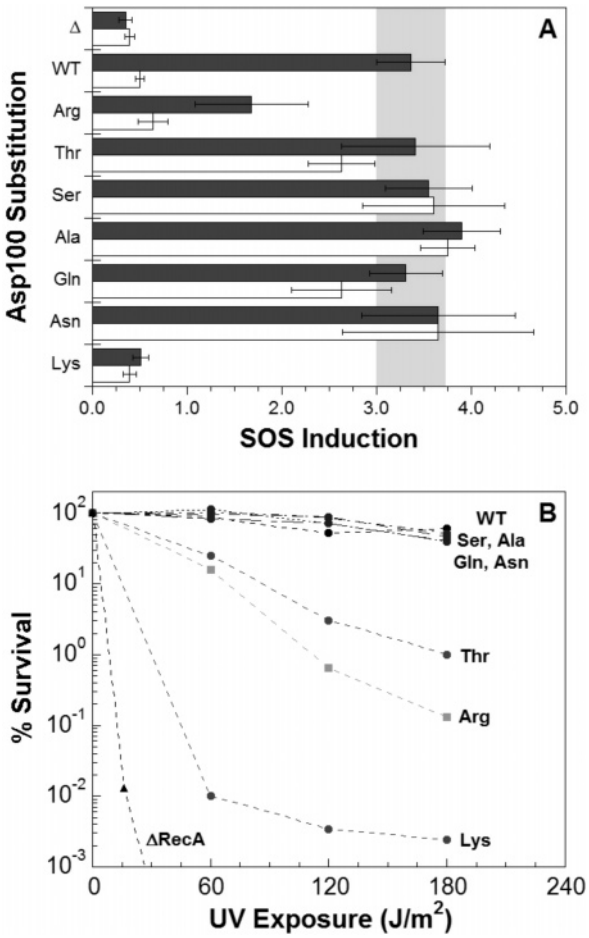

FIGURE 2: In vivo characterization of a small Asp100 mutant RecA library. (A) SOS induction by Asp100 mutants. The induction of the SOS response, measured by β-galactosidase activity, is shown for the Asp100 mutants in both the presence (dark gray bars) and absence (white bars) of the DNA-damaging antibiotic Mitomycin C (0.5 μg·mL^{-1}). The amino acid substitution made at position 100 is indicated by the three-letter amino acid code below the horizontal axis. Δ indicates the *recA*$^-$ control, where the plasmid vector was inserted into the cells with no RecA present. Error bars are calculated as the standard deviation of the mean of at least three experiments for each protein. The horizontal gray bar represents the level of SOS induction by the wild-type RecA for comparison to the mutants. (B) Survival of cells containing mutant RecA proteins in the presence of UV radiation. Cells containing the proteins from the Asp100 mutant library were irradiated in 10 mM $MgSO_4$ and plated for overnight growth. Colonies were counted, and the survival was calculated as a percentage of the growth of nonirradiated cells for each RecA protein. No cell growth was observed with *recA*$^-$ cells (ΔRecA) at 8 J·m^{-2} of UV exposure, and only the first exposure point is plotted as a result.

assay, the D100R RecA promotes only 0.1% of cell survival relative to the wild-type RecA at 180 J·m^{-2} of UV irradiation. The D100K RecA protein is incapable of promoting cell survival and shows the same level of survival as a *recA*$^-$ strain after only 60 J·m^{-2} of UV irradiation. However, with the exception of the Thr100 mutant, which confers an intermediate phenotype, all the other mutant proteins exhibited a similar survival phenotype as that of wild-type RecA.

Purification of D100R RecA Protein for Biochemical Characterization. In general, a polar residue at position 100 is apparently necessary for high-level activity in vivo and in vitro. Nonpolar side-chain substitutions at Asp100 are either inactive, unstable with respect to aggregation, or both. However, polar, uncharged residues such as Ser, Thr, Asn,

and Gln, as well as Ala, all result in a constitutive coprotease phenotype. The D100N RecA protein has been biochemically characterized as more active than WT RecA in many respects, including its abilities to hydrolyze ITP with a low $S_{0.5}$, utilize ITP as an activating cofactor for strand exchange at neutral pH, and to hydrolyze ITP with minimal inhibition by SSB (*26*, *27*). Our biological activity data demonstrate that these enhancements are reflected in vivo by a constitutive coprotease phenotype. Constitutive coprotease function may indicate an altered interaction with DNA, with the LexA repressor, or both and adds a level of complexity to the studies that we did not wish to explore. Hence, we selected the D100R protein for study, because it approximates the activity of the WT protein in both the SOS induction and UV survival experiments.

To understand the molecular basis of the phenotypic difference between D100R and WT RecA, we purified both and compared their biochemical activities in vitro. We undertook a large-scale, intein-mediated, affinity-fusion purification (*29*), which has key advantages over the small-scale purifications described above. First, the large-scale purification allows for greater purification yields, in excess of 150 mg, useful for doing multiple experiments with each protein. Second, the large-scale purification includes a heparin column chromatography step, which removes at least one visible contaminant from the protein prep and results in a measurable increase in purity. The WT and D100R RecA proteins behaved similarly during the purification procedure, and both were purified to >97% homogeneity (data not shown).

D100R RecA Protein Has a Reduced Turnover Number for ATP Hydrolysis. As described above, ssDNA-dependent ATP hydrolysis serves as a useful indicator of active nucleoprotein filament formation. Therefore, we tested the ability of D100R RecA to hydrolyze ATP in the presence of ssDNA. In the first set of experiments, initial rates of ATP hydrolysis were measured using excess poly(dT) to activate either the WT or D100R RecA protein (1 μM). As shown in Figure 3A, initial hydrolysis rates for the mutant protein were substantially lower than those of WT RecA across the range of poly(dT) concentrations. Analysis of the data for WT RecA yielded $k_{cat} = 24 \pm 1$ μM·min^{-1}, a value that agrees well with that reported previously (*47*). In contrast to the data for WT RecA, the dependence of the ATP hydrolysis rates for D100R RecA on [poly(dT)] were not adequately described by eq 1. Visual inspection of the data for the D100R protein reveals a sigmoidal shape, so the D100R values were fit with eq 2, yielding $k_{cat} = 8.9 \pm 0.5$ μM·min^{-1} for D100R RecA. Although both proteins display saturation in their poly(dT)-dependent ATPase velocities, D100R RecA turns over ATP approximately 3-fold more slowly than the WT protein. The DNA-binding parameters obtained from this analysis will be discussed below.

The same trend was observed in a second set of experiments, in which ϕX174 cssDNA was titrated with RecA. In this assay, the native secondary structure in the phage DNA must be overcome by preferential binding of RecA to the single-stranded regions. At all protein concentrations, WT and D100R RecA hydrolyze ATP at significantly different rates (Figure 3B). Analysis of the data using eqs 1 and 2 as above for the WT and mutant enzymes, respectively, yielded $V_{max} = 47 \pm 3$ μM·min^{-1} for WT RecA and 10 ± 1 μM·min^{-1} for D100R RecA. Interestingly, the ATPase velocity for D100R RecA saturates well below the protein

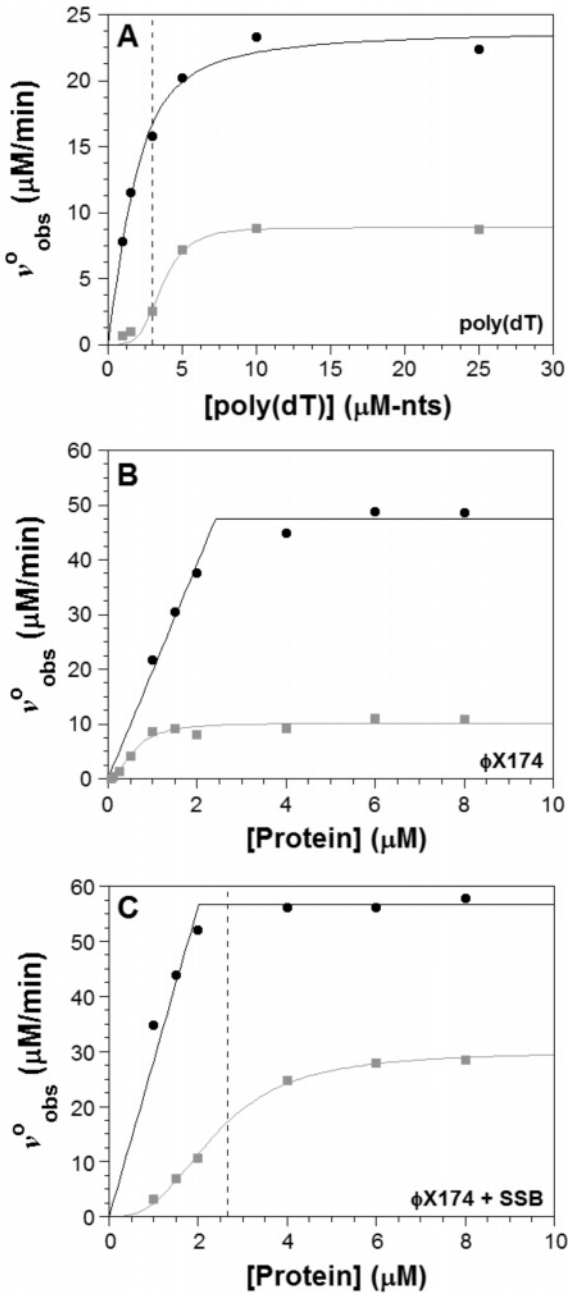

FIGURE 3: ATPase activities of WT and D100R RecA proteins. (A) Poly(dT)-dependent ATPase activity of WT and D100R proteins. Reactions were performed as described Experimental Procedures, and the data were fit to determine the relevant ATPase parameters. For the WT RecA (black circles), the data were fit with eq 1, and for D100R RecA (gray squares), the data were fit with eq 2. The dashed vertical line represents a DNA/RecA stoichiometry of 3 nts/RecA monomer. WT RecA: $V_{max} = 24$ μM·min^{-1}, $n = 2.1$, $K_d = 0.32$ μM. D100R RecA: $V_{max} = 8.9$ μM·min^{-1}, $n = 4.2$, $C_{0.5}^{DNA} = 3.6$ μM nts. (B) ssDNA-dependent ATP hydrolysis by WT and D100R RecA in the absence of SSB. Data were fit as in panel A, with $K_d = 0$ μM for the WT RecA curve fit. The ATP hydrolysis activity of WT and D100R RecA was tested using ϕX174 cssDNA in the absence of SSB. WT RecA: $V_{max} = 47$ μM·min^{-1}, $n = 3.3$. D100R RecA: $V_{max} = 10$ μM·min^{-1}, $n = 2.1$, $C_{0.5}^{DNA} = 10$ μM nts. (C) ϕX174 cssDNA-dependent ATPase activity of the WT and D100R proteins in the presence of SSB. Data were fit as in panel A, with $K_d = 0$ μM for the WT RecA curve fit. WT RecA: $V_{max} = 57$ μM·min^{-1}, $n = 4.0$. D100R RecA: $V_{max} = 30$ μM·min^{-1}, $n = 2.8$, $C_{0.5}^{DNA} = 2.4$ μM nts.

Table 1: Kinetic Parameters for Steady-State NTP Hydrolysis by WT and D100R RecA Proteins[a]

	WT RecA				D100R RecA				D100N RecA[b]			
NTP	k_{cat} (min^{-1})	$S_{0.5}$ (μM)	n_H	$(k_{cat}/S_{0.5})_{rel}$	k_{cat} (min^{-1})	$S_{0.5}$ (μM)	n_H	$(k_{cat}/S_{0.5})_{rel}$	k_{cat} (min^{-1})	$S_{0.5}$ (μM)	n_H	$(k_{cat}/S_{0.5})_{rel}$
ATP	20	50	3	1	9.9	59	3	1	18	85	3	1
dATP	22	39	3	1.4	14	44	2	2.0				
ITP	22	240	3	0.23	13	94	3	0.83	18	125	3	0.69
GTP	15	1400	5	0.03	6.4	480	4	0.08	20	215	3.5	0.44

[a] Each NTP was titrated in the presence of 0.5 mM RecA protein, and the data were fit using eq 3 to yield the k_{cat} and $S_{0.5}$ parameters. Values are the mean of three experiments, and the standard deviation was ≤10% for each value. [b] The values reported for the D100N protein are taken from work performed by Stole and Bryant (*26*) and are shown to compare the activity of a known Asp100 mutant to the D100R RecA protein.

concentration required for WT RecA (<1 vs 3 μM, respectively).

In the presence of SSB, WT RecA is known to be activated for ATP hydrolysis by phage DNA with a slightly enhanced V_{max} (*48*). To determine whether the same was true for D100R RecA, ATPase assays with ϕX174 cssDNA as the DNA cofactor were carried out in the presence of SSB (Figure 3C). Such assays are particularly sensitive to subtle changes in the ssDNA-binding affinities and kinetics of mutant RecA proteins (*49*−*51*). In large part, the sensitivity derives from the intricate balance of intermolecular forces that modulate whether SSB stimulates RecA−ssDNA binding by removing residual secondary structure in the phage DNA or inhibits RecA−ssDNA binding by competition (*52*−*55*). Consistent with previous reports, WT RecA hydrolyzes ATP with $V_{max} = 57 \pm 5$ $\mu M \cdot min^{-1}$ in the presence of SSB, an increase of 18% compared with $V_{max} = 47$ $\mu M \cdot min^{-1}$ in the absence of SSB. In contrast, there is a remarkable increase in the ATP hydrolysis rate for D100R RecA in the presence of SSB at all enzyme concentrations tested. The maximum velocity increased approximately 3-fold in the presence of SSB, from 10 to 30 ± 1 $\mu M \cdot min^{-1}$. The extent of the SSB-dependent enhancement of the D100R RecA ATPase is inconsistent with the proportion of native secondary structure expected in ϕX174 cssDNA. The discrepancy may be accounted for by the report that SSB exerts a direct positive effect on the stabilities of RecA−ssDNA complexes and blocks the dissociation of the complexes under conditions that favor secondary structure formation in the DNA (*56*).

Impact of the D100R Mutation on the $S_{0.5}$ Values for Different NTPs. In the presence of ssDNA, D100R RecA hydrolyzes ATP at a rate that is 2−5-fold lower than that of WT RecA. Because the side chain of Asp100 contacts the bound nucleotide in cocrystal structures (*5*, *46*) and biochemical data suggests that Asp100 is important in determining NTP specificity (*26*, *27*), we anticipated that replacing Asp100 with Arg would result in altered nucleotide affinity and specificity. Therefore, we carried out steady-state kinetic experiments with D100R RecA to measure k_{cat} and $S_{0.5}$ for various NTPs. Nucleotide titrations were performed using ATP, dATP, ITP, and GTP, and the results for both proteins displayed typical Michaelis−Menten kinetics with cooperative substrate turnover (data not shown) as reported previously for WT RecA (*41*). All eight data sets were fit to a modified Michaelis−Menten equation (eq 4), and the steady-state kinetic parameters for the hydrolysis of each NTP are presented in Table 1.

Consistent with the ssDNA titrations described above, the steady-state ATP turnover number was 2-fold lower for D100R RecA than for WT RecA. Interestingly, the trends in the k_{cat} values of WT and D100R RecA for the four NTPs are identical (dATP ≅ ITP > ATP > GTP), although the actual k_{cat} values for D100R are reduced approximately 2-fold relative to WT. Likewise, the trends in the $S_{0.5}$ values for the two proteins were also identical: dATP < ATP < ITP < GTP. Notably, however, the $S_{0.5}$ value for D100R with ITP is 2.5-fold lower than that for WT RecA, and the $S_{0.5}$ value with GTP is approximately 3-fold lower. These increases in relative specificity for ITP and GTP by D100R RecA are consistent with those noted for the D100N mutant protein by Bryant and co-workers (*26*, *27*), as shown in Table 1. Thus, while both D100N and D100R RecA proteins retain an overall preference for ATP, the magnitude of the specificity is reduced by virtue of a lower $S_{0.5}$ value for ITP and GTP.

Modest Differences Observed in the Binding of MANT-ADP by WT and D100R RecA. The steady-state kinetic parameters described above suggest that D100R RecA binds ATP with similar affinity to the WT protein. However, the kinetic scheme for ssDNA-dependent ATP turnover by RecA is not simple (*57*), obscuring the relationship between K_d and $S_{0.5}$ for ATP. To evaluate the thermodynamics of nucleotide binding further, we monitored the fluorescence of the ADP analogue MANT-ADP during titration experiments using the WT and D100R RecA proteins in the absence of ssDNA (Figure 4A). Fits of the reconstructed total intensity data for the two proteins using eq 4 reveal that the K_d for MANT-ADP is only 3-fold higher for D100R RecA relative to WT RecA. The experiment was designed with the knowledge that the crystallographic structures of RecA which show protein−nucleotide interactions represent the inactive conformation of the RecA filament. This conformation is distinct from that present during ssDNA-dependent ATP turnover. Hence, the use of MANT-ADP binding to protein in its inactive state would facilitate direct comparisons with the structural data. Coupled with the observation that the emission peaks and anisotropy are not significantly different between the two proteins (see Supporting Information), the binding titration data support the conclusion that D100R RecA interacts with MANT-ADP in a manner that is structurally and energetically similar to the WT protein.

D100R RecA Has Reduced Apparent Affinity for ssDNA in the Presence of ATP. The steady-state $S_{0.5}$ parameters and MANT-ADP titration data are consistent with the conclusion that the WT and D100R RecA proteins are generally similar with respect to NTP (NDP) binding. In particular, D100R RecA hydrolyzes ATP at a slightly lower steady-state rate and interacts with NTPs with only modest alterations in affinity and specificity. In contrast, the biological activity

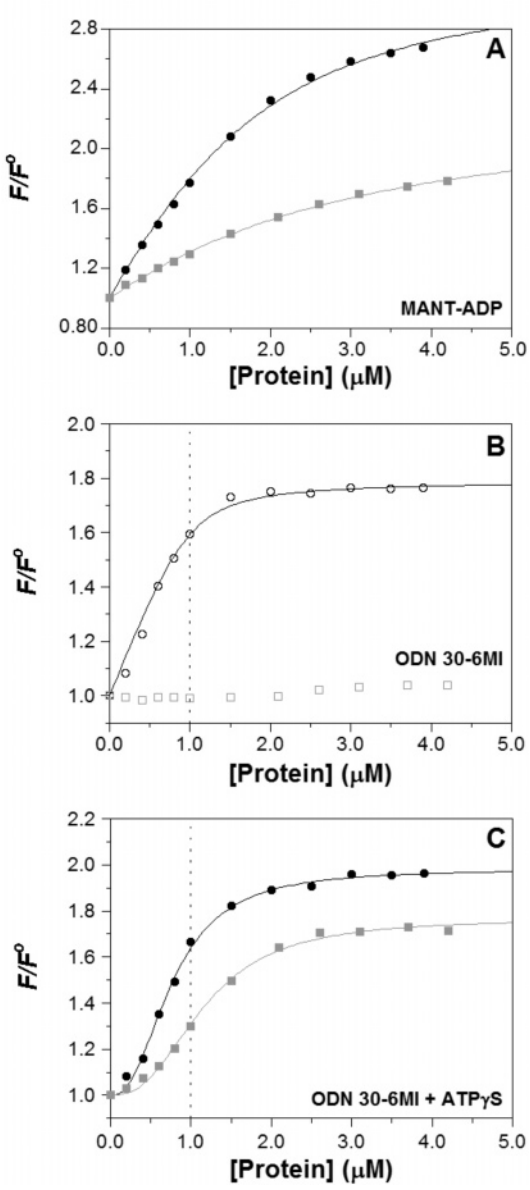

FIGURE 4: Nucleotide and ssDNA binding by the WT and D100R RecA proteins. (A) Normalized total intensity of MANT-ADP bound by WT and D100R RecA. The total intensity was normalized to the total intensity in the absence of protein and was fit using eq 5 to determine the K_d for MANT-ADP binding by each protein ($I_0 = 1$ for each fit). WT RecA: $\Delta F = 2.2$, $K_d = 0.81$ μM;. D100R RecA: $\Delta F = 1.3$, $K_d = 2.0$ μM. (B) Normalized total intensity of the RecA−ssDNA complex in the absence of nucleotide cofactor. The total intensity at each titration point was calculated and plotted for each protein to compare the binding of ssDNA (3 μM nts final) by the enhancement of the 6MI fluorescent signal. The dashed vertical line represents a binding stoichiometry of 3 nts/RecA monomer. No signal enhancement was visible upon addition of D100R protein (open gray squares). The total intensity data for the WT RecA (open black circles) was fit using eq 6 to determine the K_d for DNA binding in the absence of ATPγS cofactor: $\Delta F = 0.79$, $K_d = 0.08$ μM. (C) Normalized total intensity of the RecA−ssDNA complexes in the presence of ATPγS. The total intensity at each titration point was calculated and plotted for each protein to compare the binding of ssDNA (3 μM nts final) by the enhancement of the fluorescent signal. The dashed vertical line represents a binding stoichiometry of 3 nts/RecA monomer. As the data is sigmoidal in shape for both proteins, eq 7 was used, incorporating a cooperativity parameter, to describe the curve fit and determine the K_d and cooperativity (m) for DNA binding. WT RecA: $\Delta F = 0.98$, $K_d = 0.77$ μM, $m = 2.4$. D100R RecA: $\Delta F = 0.77$, $K_d = 1.2$ μM, $m = 2.6$.

data and the shapes of the poly(dT)- and ϕX174-dependent ATPase titration curves suggest that the amino acid substitution at position 100 markedly affected RecA protein's ability to co-process ATP and ssDNA. Because nucleotide binding and usage appeared similar for the two proteins, we investigated the DNA-binding properties of the WT and D100R protein to determine any key differences between the two.

To compare the relative abilities of ssDNA molecules to activate the RecA protein variants for NTP hydrolysis, the concentration-dependent ATPase rates (Figure 3) were further analyzed using eq 1. Because the V_{max} parameters were reported above, only the DNA-binding parameters will be described here. Analysis of the poly(dT)-dependent ATPase data for WT RecA (Figure 3A) yielded n and K_d values of 2.1 ± 0.7 nts and 0.32 ± 0.3 μM nts, respectively. Because ssDNA binding by RecA is cooperative and sequence-nonspecific, the total apparent affinity has two contributions, intrinsic affinity (K) and cooperativity (ω), and $K_d = (K\omega)^{-1}$ (*12*, *58*). Typically, however, observations related to ssDNA binding by RecA do not reveal this cooperativity (*47*), presumably because either the solution conditions result in stoichiometric binding (*12*) or the extent of RecA self-association mitigates the measured cooperativity in ssDNA binding (*58*). Consistent with this fact, the plot for WT RecA (Figure 3A) does not exhibit a cooperative appearance.

In contrast to the data for WT RecA, the poly(dT)-dependent ATPase data for D100R RecA clearly exhibit a sigmoidal appearance (Figure 3A), and eq 1 could not be used to fit these data adequately. The equation, $v_{obs}{}^0 = V_{max}\cdot[DNA]\cdot(C_{0.5}{}^{DNA} + [DNA])^{-1}$, was used previously to describe initial ssDNA-dependent ATPase rates catalyzed by WT RecA (*47*). In the equation, $C_{0.5}{}^{DNA}$ is the concentration of DNA required for half-maximal velocity, and in the absence of cooperativity, $C_{0.5}{}^{DNA}$ is equivalent to the apparent dissociation constant for DNA, $K_d{}^{app}$. Modification of this equation to allow for cooperativity in RecA−poly(dT) binding gave eq 2, where n is a cooperativity coefficient. Analysis of the data for D100R RecA using eq 2 yielded $C_{0.5}{}^{DNA}$ and n values of 3.6 ± 0.3 μM nts and 4 ± 1 nts, respectively. By comparison, fitting the data for WT RecA using eq 2 gave a theoretical curve with $C_{0.5}{}^{DNA} = 1.6 \pm 0.3$ μM nts and $n_H = 1.5 \pm 0.3$ nts that was indistinguishable in shape from that obtained using eq 1. This $C_{0.5}{}^{DNA}$ value for WT RecA is essentially the same as $K_d{}^{app} = 1.8$ μM reported previously (*47*).

To evaluate further the influence of the D100R change on RecA−DNA interactions, we analyzed the ϕX174 css-DNA-dependent ATPase titration curves as described above. Because WT RecA−cssDNA binding is essentially stoichiometric under the conditions of the ATPase measurement, the concentration-dependent ATPase rates were fit using eq 1 with $K_d \equiv 0$ and V_{max} and n as adjustable parameters. Analysis of the data for WT RecA gave $n = 4.0 \pm 0.3$ nts (Figure 3B).

Like the observation described above for the poly(dT) titration data, the ϕX174 cssDNA-dependent ATPase data for D100R RecA exhibit a sigmoidal appearance (Figure 3B). As before, analysis of the data for D100R RecA using eq 2 yielded $C_{0.5}{}^{RecA}$ and n values of 2.4 ± 0.2 μM and 2.8 ± 0.3, respectively. By comparison, fitting the data for WT RecA using eq 2 gave $C_{0.5}{}^{RecA} = 0.86 \pm 0.5$ μM and $n = 2.2 \pm 0.4$ (not shown).

Table 2: ATPase Parameters for WT and D100R RecA Proteins with Short Oligonucleotide Substrates[a]

	WT RecA (eq 1)			WT RecA (eq 2)			D100R RecA (eq 2)		
DNA	V_{max} (μM·min^{-1})	K_d (μM)	n	V_{max} (μM·min^{-1})	$C_{0.5}^{DNA}$ (μM)	n	V_{max} (μM·min^{-1})	$C_{0.5}^{DNA}$ (μM)	n
poly(dT)	23 ± 1	0.09 ± 0.03	3	24 ± 1	1.5 ± 0.2	1.6	9.2 ± 0.7	3.3 ± 0.5	2.3
ss60	20 ± 1	0.41 ± 0.03	3	20 ± 1	2.5 ± 0.3	1.3	7.4 ± 2.0	13 ± 15	0.6
ss30	18 ± 3	20 ± 4	3	27 ± 18	140 ± 180	0.9	6.9 ± 5.0	320 ± 470	0.8

[a] Parameters shown are obtained from fits of ATPase data with either eq 1 (for WT RecA only) or eq 2 (WT and D100R RecA). For the fit of WT RecA with eq 1, the [DNA]/[RecA] stoichiometry was fixed at 3:1.

D100R RecA Does Not Bind 30-nt ssDNA in the Absence of ATP(γS). The steady-state kinetic parameters describing the ATPase activity of D100R RecA suggest that its ability to bind ssDNA is different from that of the WT protein. To characterize the intrinsic DNA binding ability of D100R RecA, we used spectrofluorometric titrations of a 30mer ODN containing the fluorescent base analogue 6MI in place of a single guanine. Recently, we demonstrated that this ODN was sufficient for definitively characterizing the assembly and activation of RecA−ssDNA complexes (*20*). The intrinsically fluorescent ODN demonstrated features characteristic of DNA bound by the RecA protein and allowed the structurally distinct nucleoprotein filaments formed in the absence and presence of ATPγS (an analogue of ATP that is hydrolyzed to a negligible extent in these experiments) to be differentiated. Therefore, we tested the binding of the WT and D100R proteins to the same 6MI-labeled 30mer used previously.

Figure 4B shows the steady-state fluorescence emission changes of ODN 30-6MI in the presence of WT and D100R RecA. Upon WT RecA addition to ODN 30-6MI, an approximately 2-fold enhancement of the ODN's emission was observed. D100R RecA does not bind the ODN in the absence of nucleotide, as the fluorescence emission does not change upon addition of protein. These changes, or lack thereof, were substantiated by similar trends in the anisotropy data (see Supporting Information).

D100R RecA Has Reduced Affinity for 30-nt ssDNA in the Presence of ATPγS. We further tested the WT and D100R RecA-binding of the ODN 30-6MI in the presence of ATPγS (Figure 4C), which maintains the active conformational state of the RecA−DNA filament. In the presence of WT RecA and ATPγS, the fluorescence intensity of the ODN 30-6MI emission is increased approximately 2-fold over the titration range. When ATPγS is present, D100R RecA is capable of binding to the ODN, as the fluorescence enhancement of 6MI in the presence of D100R RecA is similar to that observed for WT RecA. Both emission intensity and fluorescence anisotropy measurements (see Supporting Information) as a function of RecA concentration demonstrate saturating signal changes, substantiating the conclusion that the emission intensities provide an authentic signal for complex formation.

Despite the similar increases in fluorescence intensity, the binding of ODN 30-6MI by the two proteins is different. The total emission intensity observed in the presence of D100R RecA is approximately 10% weaker than that observed with WT RecA. In the presence of ATPγS, titration of 30-6MI with either WT or D100R RecA produced association isotherms that are clearly sigmoidal in appearance (Figure 4C). Indeed, an eq 5 derived from the mass balance equations for RecA−ssDNA association could not be used to fit these data adequately. Nevertheless, a higher D100R RecA concentration is required to saturate the DNA-derived fluorescence intensity changes. In addition, the apparent K_d for DNA is 10-fold greater for D100R RecA than for WT RecA in fits of corresponding anisotropy data (0.2 vs 0.02 μM, respectively; see Supporting Information), providing further evidence that the substitution of Arg for Asp100 perturbs RecA−ssDNA interactions.

D100R RecA Does Not Utilize Oligonucleotide Substrates for ATPase Activity as Effectively as WT RecA. The DNA-dependent ATPase and 30-6MI spectrofluorometric titration data suggest that WT and D100R RecA are quantitatively different with respect to ssDNA binding. However, poly(dT) and ϕX174 DNA binding by WT RecA are essentially stoichiometric and, in the context of 30-6MI binding, ATPγS is known to stabilize RecA−DNA complexes. To explore the influence of the D100R change on RecA−DNA binding, we examined the activation of the protein's ATPase activities by relatively short ODNs. These ODNs were a nonfluorescent 30mer, identical in sequence to the one utilized above, and a 60mer from which the 30-nt sequence is derived. We have previously used these ODNs to characterize both ssDNA binding by WT RecA and the activation of its ATPase activity by short DNA lattices (*59*). The data obtained with these substrates recapitulates the trend observed with both poly(dT) and ϕX174 cssDNA substrates for V_{max}: D100R RecA exhibited a lower V_{max} with all the DNA cofactors (Table 2; see Supporting Information for plots of data). As with the longer DNA molecules, the data sets for D100R could not be fit with eq 1, as they exhibit sigmoidal appearances. While the K_d values increase with decreasing DNA length, all of the DNA molecules are able to fully activate both WT and D100R RecA. These observations substantiate the hypothesis that the D100R mutation effects a change in the interaction between RecA and ssDNA, manifested in a reduction in the activation of the D100R RecA ATPase with all DNA substrates from 30mer ODNs to phage ssDNA.

D100R RecA Does Not Compete with WT RecA for Binding to ϕX174 cssDNA. Taken together, the data presented to this point reveal deficits in the abilities of D100R RecA to turn over NTPs as hydrolytic substrates (V_{max}) and to bind ssDNA (K_d and $C_{0.5}^{DNA}$). The ATPase and DNA-binding activities of RecA are interrelated (*24*) and highly cooperative (*60*). It is possible that D100R RecA would act as a modulator of the WT RecA's activity in the context of filaments containing both proteins simultaneously. Alternately, WT RecA could serve to activate the impaired functions of D100R RecA. To test the activity of mixed filaments formed by D100R and WT RecA, mole-fraction

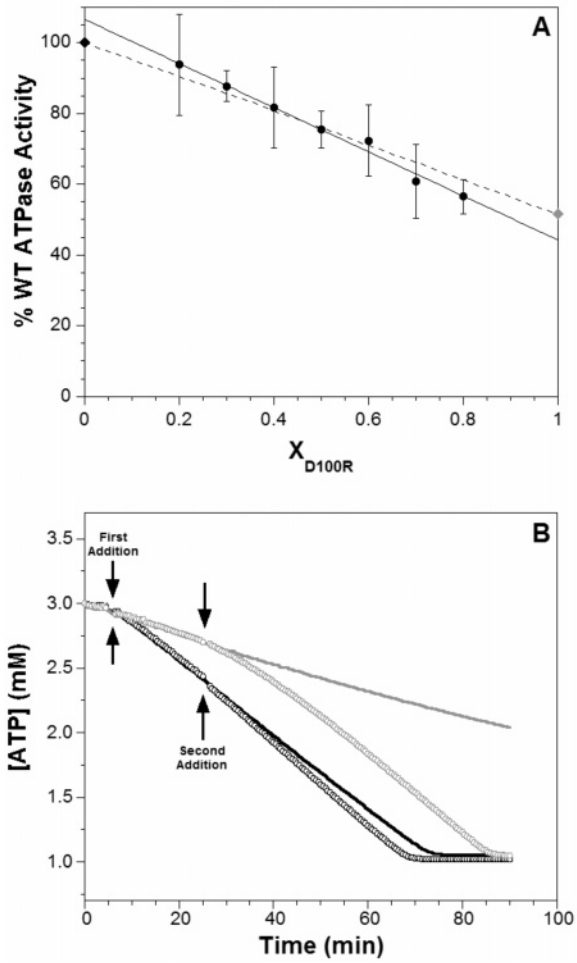

FIGURE 5: Effects of mixing WT and D100R RecA on the rates of ATP hydrolysis. (A) The percentage of WT ATPase activity in the presence of excess ϕX174 cssDNA is shown here for different ratios of WT and D100R RecA. The dotted line indicates the linear trend from 100% WT RecA (57 μM·min^{-1}) to 100% D100R RecA (30 μM·min^{-1}). (B) The hydrolysis of ATP upon addition of WT or D100R RecA is shown. The arrows indicate the points at which protein was added. The reactions were started by the addition of one of the two proteins (first addition) and were subsequently challenged with the other protein (second addition) at an equal concentration. The conditions are as follows: 2 μM WT only, black line; 2 μM D100R only, gray line; 2 μM WT + 2 μM D100R, black circles; 2 μM D100R + 2 μM WT, gray circles.

titration experiments were performed in which the aggregate ATPase activity was measured in the presence of excess ϕX174 cssDNA (Figure 5A). The mole fraction of D100R RecA was continuously varied at a constant total protein concentration such that the trend from 100% WT ($x = 0$) to 100% D100R protein ($x = 1$) was monitored. Within error, the trend in the ATPase activity was the same as the trend expected for the case where the protein activities are simply additive (dotted line). In the presence of excess ssDNA, D100R RecA was not inhibitory to WT RecA and WT RecA was not stimulatory to D100R RecA. In the case where DNA is limiting, a different result was obtained. As shown in Figure 5B, addition of WT to D100R protein causes an increase in the velocity to that comparable to WT alone. Conversely, addition of D100R to WT RecA does not cause any significant change in the observed ATPase velocity. Taken together, these results show that WT RecA outcompetes D100R RecA for filament formation on ssDNA.

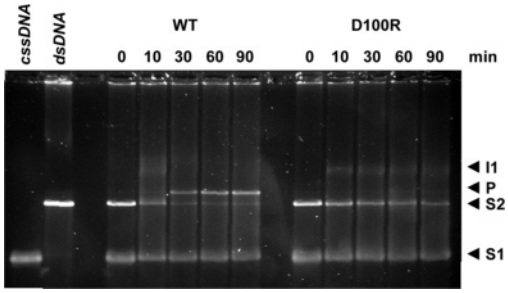

FIGURE 6: ATP-dependent strand exchange reactions with WT and D100R RecA. The reactions were initiated by addition of SSB and ATP to a solution containing 10 μM RecA protein and 20 μM nts each of ϕX174 cssDNA and ϕX174 dsDNA linearized by *Xho*I digestion. The reactions were stopped at the indicated times and analyzed by agarose gel electrophoresis. S1 = cssDNA substrate; S2 = linear dsDNA substrate; I1 = partially exchanged strand exchange intermediate; P = nicked circular dsDNA product. The slight change in the apparent band intensities from left to right across the image resulted from a combination of nonuniformity in the UV lamp of the transilluminator and a modest amount of sample precipitation during the longer incubation times.

D100R RecA Is Impaired for Catalysis of DNA Three-Strand Exchange. The RecA-mediated DNA three-strand exchange reaction between a ssDNA and a dsDNA serves as an in vitro model for the physiologic recombinational functions of the protein (*4*). DNA strand exchange is mediated by three activities of the active nucleoprotein filament: an initial sequence-nonspecific binding of dsDNA, the sequence-dependent alignment of complementary strands from the two DNA substrates, and branch migration. Deficiencies in any of these activities by the mutant nucleoprotein filament would be revealed by an altered DNA strand exchange activity. To compare D100R RecA with WT RecA, we performed typical DNA strand exchange assays (Figure 6). In the assays, a ϕX174 cssDNA molecule and a linear ϕX174 dsDNA molecule are recombined to form a nicked circular dsDNA molecule and a linear ssDNA molecule, all of which are readily separated by agarose gel electrophoresis. The WT RecA forms a significant level of joint molecule intermediates in which all the strands are bound to RecA, after just 10 min, and essentially completes the strand exchange reaction after 60 min. In contrast, the D100R protein never forms any discernible nicked circular dsDNA product. It is clear that D100R binds to both the ssDNA and dsDNA substrates and brings them together, as levels of joint molecule intermediates build up over the time course of the reaction. However, D100R RecA was unable to resolve the joint molecules into a strand-exchanged product, even after 90 min of incubation.

To tease out the basis for this mutational effect, we carried out the reaction with ATPγS in place of ATP. For WT RecA, ATPγS stimulates the high-affinity DNA binding conformation and promotes dsDNA uptake into the filament but blocks full strand exchange. The formation of joint molecule intermediates in the presence of ATPγS by WT RecA and D100R RecA was essentially identical and similar to that observed in the reaction promoted by D100R RecA with ATP (see Supporting Information). We have shown that, under conditions favorable for strand exchange, the D100R protein hydrolyzes ATP (Figure 3B) and binds DNA in an active conformation (Figure 4C), so the lack of strand exchange products cannot be solely attributed to a loss of either of these two properties.

DISCUSSION

The principal conclusion of this study is that alteration of the ATP-binding site of RecA by substitution of arginine for aspartate at position 100 causes a surprisingly modest perturbation of protein−ATP interactions and an unexpected and significant decrease in the affinity of the protein for ssDNA. Physiologically, D100R RecA was characterized by an inducible, albeit reduced, activation of the SOS response and a diminished ability to promote cellular survival after UV irradiation. The biochemical bases of these in vivo activities were revealed by in vitro activity assays. In the absence of DNA, spectrofluorometric titrations of D100R and WT RecA with MANT-ADP suggested that ADP binding is not substantially altered by the D100R change. In the absence of ATP(γS), however, ODN 30-6MI does not bind to D100R RecA. Assays conducted in the presence of both ATP and ssDNA confirmed that the more substantial mutational effect was on DNA binding rather than ATP binding. In ATPase assays with poly(dT) as the activating DNA, no changes in the $S_{0.5}$ or n_H kinetic parameters for ATP were measured, and only modest increases in the specificity constants for the nonpreferred substrates GTP and ITP were observed. Spectrofluorometric titrations of WT and D100R RecA with 30-6MI in the presence of ATPγS revealed a decreased affinity of the mutant protein for the 30mer. This mutational effect on DNA binding was corroborated by the decreased [DNA]-dependent activation of D100R RecA ATPase activity in the presence of 30- and 60mer ODNs as well as poly(dT) and ϕX174 DNA.

When measured individually, the quantitative mutational perturbations of ATP- and DNA-binding by RecA are unexceptional. Nevertheless, the results of the UV survival assay, which is an indicator of aggregate activity, revealed a more dramatic deficit arising from the D100R substitution. The in vivo activity of D100R RecA better corresponds to the following in vitro observations: (1) a 2−5-fold decrease in steady-state turnover of ATP; (2) no formation of mixed nucleoprotein filaments when WT and D100R RecA compete for limiting ssDNA; and (3) no formation of strand exchange reaction products. Taken together, these results suggest that the D100R mutational effects on isolated RecA activities combine synergistically to perturb its higher order functions. As discussed below, we hypothesize that the electrostatic potential created by the negatively charged Asp100 regulates NTP selectivity and the transduction of ATP binding into conformational activation for DNA binding and higher-order processing.

Influence of Replacing Asp100 with Arg on NTP Binding and Hydrolysis. The steady-state turnover number for ATP hydrolysis by D100R RecA was 2−5-fold lower than that for WT RecA. Crystallographic (*5*, *46*) and biochemical (*26*) data indicate that the side chain of Asp100 contributes to the ATP-binding site of RecA. Indeed, its presumed role in modulating the affinity and specificity for NTPs initially led us to explore substitutions at Asp100. The simplest interpretation of the kinetic impact of the D100R substitution is that changes in side chain−nucleotide interactions lead to a reduction in the rate of chemical reaction at the ATPase site. However, this interpretation is not sufficient to account for all the results, as will be discussed below.

First, in the crystal structures of the RecA·ADP (*5*) and RecA·AMP-PNP (*46*) complexes, the Asp100 side chain contacts the Hoogsteen pairing edge (i.e., N^6 and N^7) of the adenine moiety and is remote from the location of the β- and γ-phosphoryl moieties. The presumed hydrogen bonds with the adenine base were taken advantage of in the design of the D100N RecA protein (*26*). Because the Asp100 side chain is not in close proximity to the site of ATP hydrolytic chemistry, it would not be expected to participate directly in the chemical transformation.

Second, although the structural analysis suggests that altering the functional groups present at residue 100 would alter RecA's affinity for ATP, D100R RecA does not exhibit an increase in the concentration required for half-maximal ATPase velocity ($S_{0.5}$). Indeed, the $S_{0.5}$ values for the hydrolysis of both ATP and dATP by the WT and D100R RecA proteins are identical within experimental uncertainty, while the $S_{0.5}$ values for the hydrolysis of GTP and ITP are 2−3-fold lower for the mutant enzyme (Table 1). Moreover, as described above, there is an exact correspondence between the trends in the NTP-specific k_{cat} and $S_{0.5}$ values observed for WT and D100R RecA. These observations do not support the conclusion that substituting Arg for Asp100 has a direct influence on ATP hydrolysis or its binding during steady-state turnover.

Third, examination of nucleotide binding by the two proteins using the binding-sensitive fluorescence of MANT-ADP revealed only modest differences between the two RecA·MANT-ADP complexes. Using fluorometric titrations (Figure 4A), we found only a small difference in the K_d for MANT-ADP binding between WT RecA and D100R RecA. The results from the binding studies imply that WT RecA and D100R RecA bind MANT-ADP in similar fashion and that the arginine substitution at position 100 does not affect the ATP-binding site of RecA to a remarkable extent.

On the basis of the cocrystal structures of RecA with adenosine nucleotides and the Bryant laboratory's observations on D100N RecA, our simple expectations were that the D100R substitution would influence ATP binding affinity and selectivity. Contrary to expectation, however, the accumulated evidence leads to the inference that the altered activity of D100R results not from a simple change in nucleotide binding but rather from a change in the ability of the protein to transduce ATP binding into conformational activation for DNA binding.

Influence of Replacing Asp100 with Arg on ssDNA Binding. Measuring the rates of ATP hydrolysis under steady-state conditions in the presence of either poly(dT) or ϕX174 cssDNA as the activating cofactor revealed that, while the titration data for WT RecA are well-described by a simple rectangular hyperbola, the data for D100R RecA exhibit a pronounced sigmoidal shape. Although the extraction of thermodynamically rigorous DNA-binding parameters from such indirect assays is complicated, we can infer that DNA binding is quantitatively different for the two proteins. This conclusion is supported by the clear difference between WT and D100R RecA with respect to binding the intrinsically fluorescent 30-nt DNA. In the absence of ATP(γS), the D100R protein does not appear to bind ODN 30-6MI at all (Figure 4B). In the presence of ATPγS, D100R is activated for 30-6MI binding. However, the binding of the proteins to DNA is notably different, as the WT protein clearly

saturates the DNA at a lower concentration than the D100R protein (Figure 4C).

The conclusion that the DNA-binding ability of D100R RecA is less than that of WT RecA is further corroborated by the effects of competition and SSB on the ATPase results. We have shown that, while D100R RecA does catalyze ATP hydrolysis, WT RecA appears to dominate filament formation and ATP hydrolysis when both proteins are present with limiting ssDNA. In the context of ϕX174-dependent ATPase activity, SSB has a dramatic effect on catalysis by D100R RecA: the maximum velocity is more than 3-fold higher in the presence of SSB than in its absence. Cox and co-workers established that SSB exerts a direct positive effect on the stability of RecA−ssDNA complexes and blocks the dissociation of RecA−ssDNA complexes under conditions that favor the formation of secondary structure in ssDNA (*56*). These conclusions are consistent with the hypothesis that D100R RecA forms a relatively unstable nucleoprotein filament, resulting in an apparent decrease in all DNA-associated activities relative to those of WT RecA.

Taken together, the observations that D100R RecA can be readily displaced from its nucleoprotein filament by WT RecA, while the same filament can be stabilized by SSB, suggest that D100R RecA forms a kinetically labile filament on ssDNA. Two related observations further support the conclusion that the defect results from a shorter dissociative lifetime rather than a slower rate of filament formation. Slower filament formation kinetics are manifest in a reduced ability to compete with SSB for ssDNA (*50*, *61*) and can be readily observed using stopped-flow spectrofluorometry with ODN 30-6MI (*20*). Although a full discussion of association−dissociation kinetics is beyond the scope of this report, preliminary experiments to date, using both types of assays, have failed to reveal a dramatic defect in the kinetics of nucleoprotein filament formation by D100R RecA.

RecA Uses Coulomb Forces for NTP Specification. The Bryant laboratory first described the D100N RecA protein and its increased specificity for ITP (*26*). They further noted that D100N RecA utilizes ITP as a cofactor for DNA three-strand exchange more effectively than WT RecA (*26*, *27*). On the basis of these observations, they reasoned that the D100N protein underwent a switch in cofactor specificity from ATP to ITP due to the asparagine hydrogen bonding with the inosine 6-carbonyl in the active site. In contrast, our results with D100R RecA demonstrate that its altered ATPase activity relative to the wild-type protein does not simply reflect a reduced affinity for ATP or an alteration of the cofactor specificity.

Through an elegant series of papers over the past decade, the Bryant laboratory has established a quantitative linkage between the $S_{0.5}$ value of a particular NTP and the stability of the active conformational state of the corresponding nucleoprotein filament (*24*, *26*, *27*, *62*−*64*). In this context, we note that the $S_{0.5}$ values for GTP and ITP are reduced 2.5-fold relative to the values for WT RecA by the substitution of Arg for Asp at position 100. On the basis of the similarity of these changes to those reported for D100N RecA (see Table 1), we would expect D100R RecA to use ITP as a strand exchange cofactor if the Asp-to-Arg change at position 100 resulted merely in a NTP specificity switch. However, while D100N RecA efficiently uses ITP as a cofactor for DNA three-strand exchange (*26*, *27*), D100R RecA is unable to do so (see Supporting Information). Hence, an $S_{0.5}$ value at or below 100 μM is a necessary, but not a sufficient, condition for full activity.

Taken together, the $S_{0.5}$ values of GTP and ITP with the D100N and D100R RecA proteins suggest that a mutation at position 100 does not simply alter the specificity of RecA for a particular NTP. Instead, the $S_{0.5}$ values for all NTPs except ATP (dATP) are lowered, making the enzyme more promiscuous with respect to NTP binding and usage. Nucleotide-binding sites in proteins lack specific residue conservation within the sites; rather, the binding sites are characterized by commonalities in the general shape, size, and electrostatic potential pattern among proteins that selectively bind a particular substrate (*65*−*68*). We speculate that RecA takes advantage of the negatively charged side chain of Asp100 to create an electrostatic potential pattern that discriminates against GTP (and ITP) binding and usage. The removal of the negative charge by replacing Asp with either Asn or Arg would therefore reduce the apparent selectivity for ATP by modulating the discrimination against GTP (and ITP).

RecA Uses Coulomb Forces to Transduce NTP Binding for the Protein Conformational Changes and DNA Binding Required for Active NPF Formation. Our hypothesis that the electrostatic potential created by the negatively charged Asp100 regulates NTP selectivity has further implications in light of the structural model for the active, extended RecA filament first proposed by Egelman and Campbell and their co-workers (*25*). A remarkable feature of the model is the reorientation of RecA monomers with respect to their crystallographic locations such that the ATP binding site is now located between adjacent monomers and comprises highly conserved residues on both subunits. Many important aspects of the model, including the ATP-site location at the subunit interface, have been substantiated by analyses of the crystal structures of RecA homologues in extended filaments (*18*, *46*, *69*). We reconstructed the VanLoock et al. model using the reported C_α coordinates as a template for the 1.9 Å structure of RecA bound to Mg·ADP recently reported by Xing and Bell (*46*) (Figure 7).

The active filament structural model predicts that the residues that come into close proximity to the ATP binding site upon activation are predominantly positively charged; specifically, Lys216, Arg222, Lys248, and Lys250 are implicated. The changes in the positions of these residues can be appreciated by comparison of Figure 7A (inactive filament crystal structure) with Figure 7C (active filament model). In the inactive filament structure, the ATP binding site readily accommodates either Asp or Arg at position 100 (Figure 7, panels A and B, respectively). However, substitution of Arg at position 100 in the active filament (Figure 7D) creates the potential for steric clashes with the Lys and Arg residues that have moved into position to interact with the bound nucleotide. More importantly, the substitution of Arg for Asp100 dramatically influences the electrostatic potential of one RecA monomer near the site of monomer−monomer approximation and ATP binding in the active filament (Figure 7E,F). This perturbation was revealed by the following virtual procedure: separation of the two adjacent monomers whose interface constitutes the ATP binding site in the active filament model, rotation of one of the monomers 180° around the long axis of the filament,

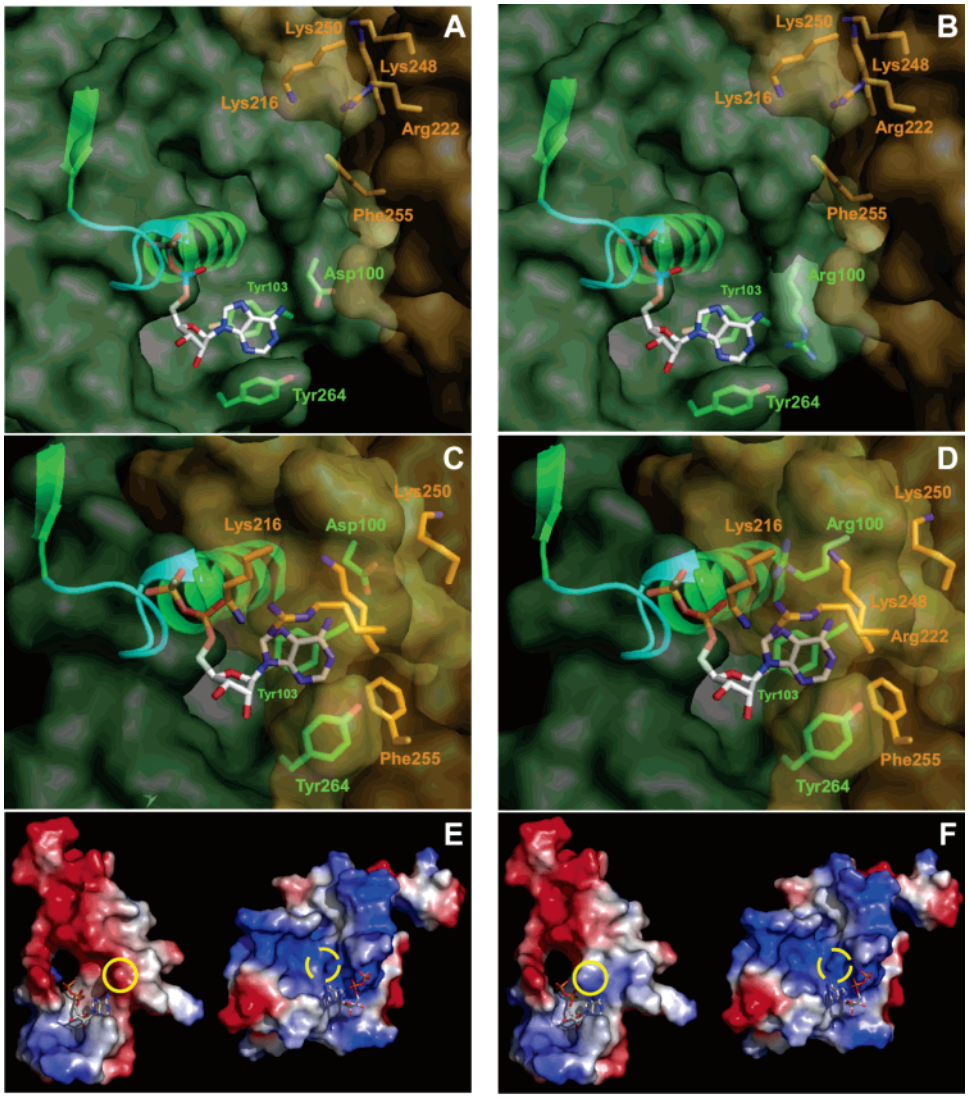

FIGURE 7: Structural model of the interaction of Asp100 and Arg100 with adjacent RecA monomers during filament assembly. The interface between monomers in the inactive form is shown for the WT RecA and the D100R RecA proteins (A and B, respectively). The P-loop is illustrated as a cyan ribbon, and the ADP is shown in CPK colors. Residues within the same monomer as the bound ADP are shown in green, and residues in the adjacent monomer are shown in orange. Note that there is a large separation between the residues within the nucleotide binding site of one monomer and the interacting residues of the adjacent monomer. The arginine mutation was made in silico and placed in one of many possible conformations within the structure. The residues involved in interactions with the nucleotide binding site of the WT RecA and the D100R RecA are shown in panels C and D, respectively. Here, the residues in the adjacent monomer have rotated down and are in proximity to the nucleotide binding site. The bottom pictures show an electrostatic map of the interface region between the two monomers for both WT RecA (E) and D100R RecA (F). The left half of each picture is the ADP-bound monomer, and the right half is the adjacent monomer. The yellow circles denote the position of the aspartate in the ADP-bound monomer and the corresponding position on the adjacent monomer where the aspartate would reside when the monomers are brought together. Note the change in the bottom picture from red to blue within the yellow circle on the left in panel F, indicative of a change from aspartate to arginine within the model.

and computation of the molecular electrostatic surface potential for each of the monomers. The procedure exposes the interface between the monomers that is obscured in the active filament model and elucidates the change from attractive Coulomb forces between WT RecA monomers to repulsive Coulomb forces for D100R RecA (Figure 7, panels E and F, respectively; note the regions indicated by yellow circles). In the context of the VanLoock et al. model for the active filament, the substitution of Arg for Asp100 clearly perturbs the steric and electrostatic complementarity between adjacent RecA monomers constituting the ATP binding site.

Molecular Basis of Mutational Effects at Asp100: The Importance of a Negative Charge. We have conjectured that Coulomb forces associated with the negative charge on Asp100 are used by RecA for the joint purpose of NTP selectivity and NTP-dependent conformational activation. This provides an attractive rationale for the structural determinants of these functional characteristics. In addition to its functions that involve motor activities, the activated nucleoprotein filament of RecA plays roles in at least one other distinct class of physiologic function. This class involves signaling activities, such as SOS induction following DNA damage (*70*) and activation of translesion DNA synthesis (*71*). RecA's biological function to induce and potentiate the SOS response to DNA damage requires that the conformational state of the nucleoprotein filament be reversible. In this context, the hypothesis that Coulomb forces associated with the negative charge on Asp100 are important

for RecA activities may provide an explanation for the mutational effects observed when the anionic Asp100 is changed to a cationic Arg. Indeed, there is an apparent requirement for a negatively charged residue at position 100 to allow for optimal protein function, as nonpolar residues severely curtailed the ability of RecA to induce SOS and DNA repair functions, while polar, uncharged residues resulted in a constitutive SOS phenotype.

CONCLUSION

In summary, we have reported that alteration of the ATP-binding site of RecA by substitution of Arg for Asp at position 100 causes a surprisingly modest perturbation of protein−ATP interactions and an unexpected and significant decrease in the affinity of the protein for ssDNA. The D100R mutational effects on individual RecA activities combine synergistically to perturb its higher-order functions. As a direct consequence of the cooperative nature of RecA−ATP and RecA−ssDNA interactions, this synergism can be rationalized by the observation that the substitution of Arg for Asp100 clearly perturbs the steric and electrostatic complementarity between adjacent RecA monomers constituting the ATP binding site in the active nucleoprotein filament. We hypothesize that Coulomb forces between adjacent filament subunits, dominated by the negatively charged Asp100 residue of one RecA monomer and the positively charged Lys and Arg residues of its neighbor, regulate the transduction of ATP binding into conformational activation for DNA binding and higher-order processing. RecA may further utilize the negatively charged side chain of Asp100 to create an electrostatic potential pattern that discriminates against GTP (and ITP) binding and usage. These studies provide insight into the interdependence of structural and functional aspects of RecA conformational activation and may be important for understanding strategies by which electrostatic potentials are used by motor proteins for long-range protein conformational changes.

ACKNOWLEDGMENT

We thank Dr. Daniel J. Cline, Dr. Mallinath B. Hadimani, and Mr. Tim J. Wigle for stimulating discussion of the manuscript.

SUPPORTING INFORMATION AVAILABLE

Emission spectra and anisotropy data for fluorescence experiments, ATPase data for short ODN experiments, and strand exchange gels. This material is available free of charge via the Internet at http://pubs.acs.org.

REFERENCES

1. Kowalczykowski, S. C. (2000) Initiation of genetic recombination and recombination-dependent replication, *Trends Biochem. Sci. 25*, 156−165.
2. Lusetti, S. L., and Cox, M. M. (2002) The bacterial RecA protein and the recombinational DNA repair of stalled replication forks, *Annu. Rev. Biochem. 71*, 71−100.
3. MacFarland, K. J., Shan, Q., Inman, R. B., and Cox, M. M. (1997) RecA as a motor protein. Testing models for the role of ATP hydrolysis in DNA strand exchange, *J. Biol. Chem. 272*, 17675−17685.
4. Cox, M. M. (2003) The bacterial RecA protein as a motor protein, *Annu. Rev. Microbiol. 57*, 551−577.
5. Story, R. M., and Steitz, T. A. (1992) Structure of the recA protein-ADP complex, *Nature 355*, 374−376.
6. Story, R. M., Weber, I. T., and Steitz, T. A. (1992) The structure of the *E. coli* recA protein monomer and polymer, *Nature 355*, 318−325.
7. Abrahams, J. P., Leslie, A. G., Lutter, R., and Walker, J. E. (1994) Structure at 2.8 Å resolution of F1-ATPase from bovine heart mitochondria, *Nature 370*, 621−628.
8. Sawaya, M. R., Guo, S., Tabor, S., Richardson, C. C., and Ellenberger, T. (1999) Crystal structure of the helicase domain from the replicative helicase-primase of bacteriophage T7, *Cell 99*, 167−177.
9. Singleton, M. R., Sawaya, M. R., Ellenberger, T., and Wigley, D. B. (2000) Crystal structure of T7 gene 4 ring helicase indicates a mechanism for sequential hydrolysis of nucleotides, *Cell 101*, 589−600.
10. Skordalakes, E., and Berger, J. M. (2003) Structure of the Rho transcription terminator: mechanism of mRNA recognition and helicase loading, *Cell 114*, 135−146.
11. Egelman, E. H., and Stasiak, A. (1993) Electron microscopy of RecA-DNA complexes: Two different states, their functional significance and relation to the solved crystal structure, *Micron 24*, 309−324.
12. Menetski, J. P., and Kowalczykowski, S. C. (1985) Interaction of recA protein with single-stranded DNA. Quantitative aspects of binding affinity modulation by nucleotide cofactors, *J. Mol. Biol. 181*, 281−295.
13. Honigberg, S. M., Gonda, D. K., Flory, J., and Radding, C. M. (1985) The pairing activity of stable nucleoprotein filaments made from recA protein, single-stranded DNA, and adenosine 5′-(gamma-thio)triphosphate, *J. Biol. Chem. 260*, 11845−11851.
14. Menetski, J. P., Bear, D. G., and Kowalczykowski, S. C. (1990) Stable DNA heteroduplex formation catalyzed by the *Escherichia coli* RecA protein in the absence of ATP hydrolysis, *Proc. Natl. Acad. Sci. U.S.A. 87*, 21−25.
15. Little, J. W., Edmiston, S. H., Pacelli, L. Z., and Mount, D. W. (1980) Cleavage of the *Escherichia coli* lexA protein by the recA protease, *Proc. Natl. Acad. Sci. U.S.A. 77*, 3225−3229.
16. Roca, A. I., and Cox, M. M. (1997) RecA protein: structure, function, and role in recombinational DNA repair, *Prog. Nucleic Acid Res. Mol. Biol. 56*, 129−223.
17. McGrew, D. A., and Knight, K. L. (2003) Molecular design and functional organization of the RecA protein, *Crit. Rev. Biochem. Mol. Biol. 38*, 385−432.
18. Bell, C. E. (2005) Structure and mechanism of *Escherichia coli* RecA ATPase, *Mol. Microbiol. 58*, 358−366.
19. Cox, M. M. (1999) Recombinational DNA repair in bacteria and the RecA protein, *Prog. Nucleic Acid Res. Mol. Biol. 63*, 311−366.
20. Roca, A. I., and Singleton, S. F. (2003) Direct evaluation of a mechanism for activation of the RecA nucleoprotein filament, *J. Am. Chem. Soc. 125*, 15366−15375.
21. Lee, A. M., Ross, C. T., Zeng, B. B., and Singleton, S. F. (2005) A Molecular target for suppression of the evolution of antibiotic resistance: inhibition of the *Escherichia coli* RecA protein by N^6-(1-naphthyl)-ADP, *J. Med. Chem. 48*, 5408−5411.
22. Bianco, P. R., and Weinstock, G. M. (1998) Characterization of RecA1332 in vivo and in vitro. A role for alpha-helix E as a liaison between the subunit-subunit interface and the DNA and ATP binding domains of RecA protein, *Genes Cells 3*, 79−97.
23. Kelley De Zutter, J., Forget, A. L., Logan, K. M., and Knight, K. L. (2001) Phe217 regulates the transfer of allosteric information across the subunit interface of the RecA protein filament, *Structure (London) 9*, 47−55.
24. Katz, F. S., and Bryant, F. R. (2001) Interdependence of the kinetics of NTP hydrolysis and the stability of the RecA−ssDNA complex, *Biochemistry 40*, 11082−11089.
25. VanLoock, M. S., Yu, X., Yang, S., Lai, A. L., Low, C., Campbell, M. J., and Egelman, E. H. (2003) ATP-mediated conformational changes in the RecA filament, *Structure (London) 11*, 187−196.
26. Stole, E., and Bryant, F. R. (1996) Reengineering the nucleotide cofactor specificity of the RecA protein by mutation of aspartic acid 100, *J. Biol. Chem. 271*, 18326−18328.
27. Katz, F. S., and Bryant, F. R. (2003) Three-strand exchange by the *Escherichia coli* RecA protein using ITP as a nucleotide cofactor: mechanistic parallels with the ATP-dependent reaction of the RecA protein from *Streptococcus pneumoniae*, *J. Biol. Chem. 278*, 35889−35896.
28. Berger, M. D., Lee, A. M., Simonette, R. A., Jackson, B. E., Roca, A. I., and Singleton, S. F. (2001) Design and evaluation of a

tryptophanless RecA protein with wild-type activity, *Biochem. Biophys. Res. Commun. 286*, 1195−1203.
29. Singleton, S. F., Simonette, R. A., Sharma, N. C., and Roca, A. I. (2002) Intein-mediated affinity-fusion purification of the *Escherichia coli* RecA protein, *Protein Expression Purif. 26*, 476−488.
30. Craig, N. L., and Roberts, J. W. (1980) *E. coli* recA protein-directed cleavage of phage lambda repressor requires polynucleotide, *Nature 283*, 26−30.
31. Miller, J. H. (1992) *A Short Course in Bacterial Genetics: A Laboratory Manual and Handbook for Escherichia coli and Related Bacteria*, Vol. 2, Cold Spring Harbor Laboratory Press, Cold Spring Harbor, NY.
32. Bailone, A., Backman, A., Sommer, S., Celerier, J., Bagdasarian, M. M., Bagdasarian, M., and Devoret, R. (1988) PsiB polypeptide prevents activation of RecA protein in *Escherichia coli*, *Mol. Gen. Genet. 214*, 389−395.
33. Defais, M., Fauquet, P., Radman, M., and Errera, M. (1971) Ultraviolet reactivation and ultraviolet mutagenesis of lambda in different genetic systems, *Virology 43*, 495−503.
34. Miller, J. H. (1972) *Experiments in Molecular Genetics*, Cold Spring Harbor Laboratory Press, Cold Spring Harbor, NY.
35. Kurumizaka, H., Aihara, H., Ikawa, S., Kashima, T., Bazemore, L. R., Kawasaki, K., Sarai, A., Radding, C. M., and Shibata, T. (1996) A possible role of the C-terminal domain of the RecA protein. A gateway model for double-stranded DNA binding, *J. Biol. Chem. 271*, 33515−33524.
36. Dri, A. M., Rouviere-Yaniv, J., and Moreau, P. L. (1991) Inhibition of cell division in hupA hupB mutant bacteria lacking HU protein, *J. Bacteriol. 173*, 2852−2863.
37. Morrical, S. W., Lee, J., and Cox, M. M. (1986) Continuous association of *Escherichia coli* single-stranded DNA binding protein with stable complexes of recA protein and single-stranded DNA, *Biochemistry 25*, 1482−1494.
38. Lusetti, S. L., Voloshin, O. N., Inman, R. B., Camerini-Otero, R. D., and Cox, M. M. (2004) The DinI protein stabilizes RecA protein filaments, *J. Biol. Chem. 279*, 30037−30046.
39. Webb, M. R. (1992) A continuous spectrophotometric assay for inorganic phosphate and for measuring phosphate release kinetics in biological systems, *Proc. Natl. Acad. Sci. U.S.A. 89*, 4884−4887.
40. Neet, K. E. (1980) Cooperativity in enzyme function: equilibrium and kinetic aspects, *Methods Enzymol. 64*, 139−192.
41. Menge, K. L., and Bryant, F. R. (1988) ATP-stimulated hydrolysis of GTP by RecA protein: kinetic consequences of cooperative RecA protein−ATP interactions, *Biochemistry 27*, 2635−2640.
42. Hawkins, M. E., Pfleiderer, W., Balis, F. M., Porter, D., and Knutson, J. R. (1997) Fluorescence properties of pteridine nucleoside analogs as monomers and incorporated into oligonucleotides, *Anal. Biochem. 244*, 86−95.
43. Hawkins, M. E. (2001) Fluorescent pteridine nucleoside analogs: a window on DNA interactions, *Cell Biochem. Biophys. 34*, 257−281.
44. Cox, M. M., and Lehman, I. R. (1981) recA protein of *Escherichia coli* promotes branch migration, a kinetically distinct phase of DNA strand exchange, *Proc. Natl. Acad. Sci. U.S.A. 78*, 3433−3437.
45. Roman, L. J., and Kowalczykowski, S. C. (1986) Relationship of the physical and enzymatic properties of *Escherichia coli* recA protein to its strand exchange activity, *Biochemistry 25*, 7375−7385.
46. Xing, X., and Bell, C. E. (2004) Crystal structures of *Escherichia coli* RecA in complex with MgADP and MnAMP−PNP, *Biochemistry 43*, 16142−16152.
47. Brenner, S. L., Mitchell, R. S., Morrical, S. W., Neuendorf, S. K., Schutte, B. C., and Cox, M. M. (1987) RecA protein-promoted ATP hydrolysis occurs throughout RecA nucleoprotein filaments, *J. Biol. Chem. 262*, 4011−4016.
48. Cox, M. M., Soltis, D. A., Lehman, I. R., DeBrosse, C., and Benkovic, S. J. (1983) ADP-mediated dissociation of stable complexes of recA protein and single-stranded DNA, *J. Biol. Chem. 258*, 2586−2592.
49. Kowalczykowski, S. C. (1991) Biochemical and biological function of *Escherichia coli* RecA protein: behavior of mutant RecA proteins, *Biochimie 73*, 289−304.
50. Lavery, P. E., and Kowalczykowski, S. C. (1992) Biochemical basis of the constitutive repressor cleavage activity of recA730 protein. A comparison to recA441 and recA803 proteins, *J. Biol. Chem. 267*, 20648−20658.
51. Lavery, P. E., and Kowalczykowski, S. C. (1990) Properties of recA441 protein-catalyzed DNA strand exchange can be attributed to an enhanced ability to compete with SSB protein, *J. Biol. Chem. 265*, 4004−4010.
52. Muniyappa, K., Shaner, S. L., Tsang, S. S., and Radding, C. M. (1984) Mechanism of the concerted action of recA protein and helix-destabilizing proteins in homologous recombination, *Proc. Natl. Acad. Sci. U.S.A. 81*, 2757−2761.
53. Tsang, S. S., Muniyappa, K., Azhderian, E., Gonda, D. K., Radding, C. M., Flory, J., and Chase, J. W. (1985) Intermediates in homologous pairing promoted by recA protein. Isolation and characterization of active presynaptic complexes, *J. Mol. Biol. 185*, 295−309.
54. Kowalczykowski, S. C., and Krupp, R. A. (1987) Effects of *Escherichia coli* SSB protein on the single-stranded DNA-dependent ATPase activity of *Escherichia coli* RecA protein. Evidence that SSB protein facilitates the binding of RecA protein to regions of secondary structure within single-stranded DNA, *J. Mol. Biol. 193*, 97−113.
55. Reddy, M. S., Vaze, M. B., Madhusudan, K., and Muniyappa, K. (2000) Binding of SSB and RecA protein to DNA-containing stem loop structures: SSB ensures the polarity of RecA polymerization on single-stranded DNA, *Biochemistry 39*, 14250−14262.
56. Morrical, S. W., and Cox, M. M. (1990) Stabilization of recA protein−ssDNA complexes by the single-stranded DNA binding protein of *Escherichia coli*, *Biochemistry 29*, 837−843.
57. Stole, E., and Bryant, F. R. (1997) The rate-determining step on the recA protein-catalyzed ssDNA-dependent ATP hydrolysis reaction pathway, *Biochemistry 36*, 3483−3490.
58. Takahashi, M., Kubista, M., and Norden, B. (1987) Linear dichroism study of RecA−DNA complexes. Structural evidence and binding stoichiometries, *J. Biol. Chem. 262*, 8109−8111.
59. Singleton, S. F., Shan, F., Kanan, M. W., McIntosh, C. M., Stearman, C. J., Helm, J. S., and Webb, K. J. (2001) Facile synthesis of a fluorescent deoxycytidine analogue suitable for probing the RecA nucleoprotein filament, *Org. Lett. 3*, 3919−3922.
60. Weinstock, G. M., McEntee, K., and Lehman, I. R. (1981) Hydrolysis of nucleoside triphosphates catalyzed by the recA protein of *Escherichia coli*. Steady-state kinetic analysis of ATP hydrolysis, *J. Biol. Chem. 256*, 8845−8849.
61. Mirshad, J. K., and Kowalczykowski, S. C. (2003) Biochemical characterization of a mutant RecA protein altered in DNA-binding loop 1, *Biochemistry 42*, 5945−5954.
62. Menge, K. L., and Bryant, F. R. (1992) Effect of nucleotide cofactor structure on recA protein-promoted DNA pairing. 1. Three-strand exchange reaction, *Biochemistry 31*, 5151−5157.
63. Meah, Y. S., and Bryant, F. R. (1993) Activation of a recombinase-deficient mutant recA protein with alternate nucleoside triphosphate cofactors, *J. Biol. Chem. 268*, 23991−23996.
64. Stole, E., and Bryant, F. R. (1995) Spectroscopic demonstration of a linkage between the kinetics of NTP hydrolysis and the conformational state of the recA-single-stranded DNA complex, *J. Biol. Chem. 270*, 20322−20328.
65. Moodie, S. L., Mitchell, J. B., and Thornton, J. M. (1996) Protein recognition of adenylate: an example of a fuzzy recognition template, *J. Mol. Biol. 263*, 486−500.
66. Nobeli, I., Laskowski, R. A., Valdar, W. S., and Thornton, J. M. (2001) On the molecular discrimination between adenine and guanine by proteins, *Nucleic Acids Res. 29*, 4294−4309.
67. Denessiouk, K. A., and Johnson, M. S. (2003) "Acceptor-donor-acceptor" motifs recognize the Watson−Crick, Hoogsteen and Sugar "donor-acceptor-donor" edges of adenine and adenosine-containing ligands, *J. Mol. Biol. 333*, 1025−1043.
68. Basu, G., Sivanesan, D., Kawabata, T., and Go, N. (2004) Electrostatic potential of nucleotide-free protein is sufficient for discrimination between adenine and guanine-specific binding sites, *J. Mol. Biol. 342*, 1053−1066.
69. Wu, Y., He, Y., Moya, I. A., Qian, X., and Luo, Y. (2004) Crystal structure of archaeal recombinase RADA: a snapshot of its extended conformation, *Mol. Cell 15*, 423−435.
70. Sassanfar, M., and Roberts, J. W. (1990) Nature of the SOS-inducing signal in *Escherichia coli*. The involvement of DNA replication, *J. Mol. Biol. 212*, 79−96.
71. Goodman, M. F. (2000) Coping with replication 'train wrecks' in *Escherichia coli* using Pol V, Pol II and RecA proteins, *Trends Biochem. Sci. 25*, 189−195.

BI052296X